Electrochemical Analysis and Scanning Electrochemical Microscopy Investigations of Photosystem I

By

Gongping Chen

Dissertation

Submitted to the Faculty of the

Graduate School of Vanderbilt University

in partial fulfillment of the requirements

for the degree of

Doctor of Philosophy

in

Chemistry

May, 2013

Nashville, Tennessee

Approved:

Professor David E. Cliffel

Professor G. Kane Jennings

Professor John A. McLean

Professor Michael Stone

To my family.

ACKNOWLEDGEMENTS

This work would not have been possible without the financial support from the National Science Foundation (DMR 0907619) and the NSF EPSCoR (EPS 10040083), and the Scialog Program from the Research Corporation for Science Advancement.

There are so many people I would like to thank for their support of this dissertation and of me. I would like to first thank my advisor Dr. David E. Cliffel for giving me the guidance I needed throughout my Ph.D. study. His expertise has added brilliant creative ideas in this work. I really appreciate his patience on preparing all the recommendation letters for scholarship and job applications. I would like to thank Dr. G. Kane Jennings for his quick emails, helpful comments and perspectives that were essential to the completion of the PSI project and this dissertation. I would also like to thank Dr. McLean and Dr. Stone for serving on my committee and offering their insight and assistance. Additionally, I would like to acknowledge Dr. Juan Tuberquia, Carlos Escobar, and Darlene Gunther from the Jennings group for the preparation of gold wafer and technical discussion. I would also like to acknowledge Dr. Brian Bachmann for the generous assistance on the bacterial experiments, and Cynthia R. Mcnees from the Bachmann Lab for her appropriate suggestions on the experimental operations.

My work with a number of post-docs, graduate students, and undergraduate students during my time at Vanderbilt University was pleasure. They were good people with excellent ideas and helpful attitudes. I would especially like to thank Gabriel LeBlanc, who always provided great help and critical technical discussion, and I was lucky enough to have joined on the PSI project. I would like to thank Dr. Peter Ciesielski, Dr. Jeremy Wilburn and Fred Hijazi who lead me into the PSI field and trained me on electrochemical techniques. I would also like to thank other members of the Cliffel Group, past and present, particularly Dr. Danielle Kimmel, Dr. Leslie

Hiatt, Dr. Jennifer McKenzie, Dr. Anh Hoang, Dave Crisostomo, Evan Gizzie for your endless help, encouragement and offering editing skills to my papers.

I am thankful to my friendship with Glenna Kramer and Kerri Grove for the opportunity to survive graduate school with. There are so many nice people I have met during my graduate school years that I have not mentioned their names. Last, I would like to thank my husband for his understanding, endless love and encouragement. And my family members who have been so supportive and let me know how proud they are of me and inspire me to do better. I love you all!

TABLE OF CONTENTS

Page

ACKNOWLEDGEMENTS III
LIST OF TABLES VIII
LIST OF FIGURES IX

Chapters

I. INTRODUCTION AND BACKGROUND 1
Photosystem I (PSI) 2
Redox Mediator 6
Shewanella 7
II. EXPERIMENTAL INSTRUMENT AND ANALYTICAL METHODS 10
Preparation of Electrodes 10
PSI extraction 11
Analytical Electrochemistry 12
Cyclic Voltammetry 12
Photochronoamperometry 14
Scanning Electrochemical Microscopy (SECM) 15
Scanning Electron Microscopy (SEM)/ Energy Dispersive X-ray spectroscopy (EDX) 19
Ultraviolet-visible (UV-Vis) Spectroscopy 20
Optical Microscopy 21
III. EFFECT OF REDOX MEDIATOR ON THE PHOTO-INDUCED CURRENT OF A PHOTOSYSTEM I MODIFIED ELECTRODE 22
Experimental 24
Materials 24
PSI Extraction and Purification 25
Preparation of PSI Modified Gold Substrate Electrode 25
Mediator Preparation 26

Photoelectrochemical Characterization 26
UV-Vis Spectrometry Characterization 26
Results and Discussion 27
Effect of Redox Mediator Formal Potential on the Photocurrent Density of PSI 28
Effect of Light Absorbance of Mediators on PSI Photocurrent Density 29
Effect of Overpotential on Photocurrent 30
Mixed Mediator Systems 31
Mediator Concentration 33
Conclusions 34
Acknowledgements 35
IV. REAL-TIME DETECTION OF MULTILAYER PHOTOSYSTEM I PHOTOELECTROCHEMICAL PROPERTIES BY SCANNING ELECTROCHEMICAL MICROSCOPY 36
Experimental 39
Chemicals and Materials 39
PSI Extraction and Purification 39
Vacuum-Assisted PSI Multilayer Assembly 40
Scanning Electrochemical Microscopy 40
Results and Discussions 40
Conclusions 45
Acknowledgement 45
V. INVESTIGATION OF THE CATALYTIC ACTIVITY FOR HYDROGEN PRODUCTION ON PLATINIZED MULTIALYER PHOTOSYSTEM I FILMS WITH SCANNING ELECTROCHEMICAL MICROSCOPY 46
Experimental 48
Results and Discussion 48
Confirmation of photoreduced platinum by SEM / EDX 48
Determination of platinum particle catalytic ability for hydrogen production by SECM 50
Conclusion 55
Acknowledgement 56

VI. INVESTIGATION OF THE DISSIMILARITY METAL REDUCTION (DMR) PATHWAYS OF SHEWANELLA WITH SPATIAL RESOLUTION BY SCANNING ELECTROCHEMICAL MICROSCOPY 57
Experimental 59
Materials 59
Microbiological Methods 59
Analytical Methods 60
Results and Discussion 61
Biofilm formation 61
Identification of soluble mediator by SWV and LC-MS data showing evidence for riboflavin at the biofilm-electrode interface 61
Real-Time quantitative detection of riboflavin 63
X-scan and Approach Curve SECM experiments over masked biofilm strip showing evidence for riboflavin involved in Shewanella ET 65
Conclusions 67
Acknowledgments 68
VII. CONCLUSIONS AND FUTURE SUGGESTIONS 69
Research Summary 69
Perspectives, Future Directions and Recommendations 70
Fabrication of nanometer-sized tips to expand SECM studies 70
Computational simulations for SECM mechanism studies 72
SECM study of corrosion mechanisms 73
Integrate PSI into flexible materials 74
Combine PSI with Hydrogenase and PSII in fuel application 74
Utilization of Shewanella in microbial fuel cells 76
Future for Redox Mediator 76
Conclusions 77
REFERENCES 78
CURRICULUM VITAE 87

LIST OF TABLES

Table Page

1. Redox mediators and their properties listed in order of $E^{0'}$ 24

2. The comparison of the photocurrent density between mixed mediator systems and their individual components 33

LIST OF FIGURES

Figure Page

1. Structure Model of Plant Photosystem I. 3

2. Structure of common mediators used in the thesis. 6

3. Typical UME cyclic voltammogram. 11

4. Typical cyclic voltammogram 13

5. Schematic illustration of SECM feedback Mode and theoretical approach curves. 17

6. Schematic illustration of TG/SC mode 18

7. Raw data of photochronoamperometry performed on a PSI modified electrode using 200 μM DCPIP as the mediator. 27

8. Energy level diagram of potentials of redox species in the PSI modified electrode chemical system, and photocurrent density of each corresponding mediator at 0 mV overpotential 29

9. UV-Vis Spectra of redox mediators 30

10. Photocurrent density of redox mediators at 0, 100, and -100mV overpotential 31

11. UV-Vis Spectra of mixed redox mediators 33

12. Photocurrent density for PSI modified gold electrodes as a function of various $Ru(NH_3)_6^{3+}$ concentrations 34

13. SECM scheme for PSI and redox mediator interaction 38

14. Approach curves at various spots 42

15. Photochronoamperometry for PSI in methyl viologen solution 44

16. SEM and EDX image of platinized PSI with using NaAsc 49

17. SEM and EDX image for platinized PSI without using NaAsc 50

18. Cyclic Voltammograms recorded on 2 mm platinum disk electrode with 10 μm Pt UME 51

19. Approach Curve on bare platinum disk electrode (black line) and on platinized PSI without using NaAsc (red line) 52

20. SECM SG/TC images of platinized PSI 53

21.SECM TG/SC images of platinized PSI 54

22. SECM TG/SC images of platinized PSI without NaAsc 55

23. Chronoamperometry shows Shewanella biofilm formation in 60 min 61

24. SWV of riboflavin produced by Shewanella biofilm and in 50 μM riboflavin 62

25. LC-MS results of riboflavin produced from Shewanella biofilm after 60 min formation..... 63

26. (A) Calibration curve at various concentrations of riboflavin (5-100 μM) in Shewanella medium. (B) Plot of real-time quantitative detection of riboflavin concentration produced by Shewanella biofilm as a function of time. 64

27. Normalized current changes of an SECM x-scan over masked Shewanella biofilm in riboflavin and FcTMA solution 66

28. Approach curve represents of z-direction reduced and oxidized riboflavin over Shewanella biofilm..... 67

CHAPTER I

INTRODUCTION AND BACKGROUND

To meet the challenges of the energy shortage, climate change, and fossil fuel depletion causing pollution, alternative or renewable energy is expected to become a leading solution for energy support in the near future. While there are many types of alternative energy, solar and biofuel approaches have been considered the leading candidates based on the energy information administration 2011 report.[1] Solar energy is the most abundant energy on earth. Biological molecules, especially highly ordered proteins and microorganisms have evolved and designed through natural selection to execute complicated reactions, such as enzyme catalysis, reduction of metals, and generation of photocurrents. They are existing, readily available, biological molecular machines. The question is how to learn from these sophisticated natural structures and harness their power for human energy needs. One way is to integrate the key component of photosynthesis, photosystem I (PSI), into electronic devices to facilitate the development of solar energy applications. An additional way is to integrate the metal reducing microbe, *Shewanella*, into microbial fuel cells that will speed the expansion of biomass fuel cell energy utilization. The detailed understanding of the working mechanism and their interaction with environmental molecules will assist the utilization of bio-hybrid material.

The research presented herein focuses on using electrochemical analytical methods to study biological materials, mainly PSI and *Shewanella* bacteria, which will provide insight for daily human utilization. One of the most powerful tools used to study these materials was scanning

electrochemical microscopy (SECM), which is a robust chemical microscope with high spatial resolution, allowing real-time monitoring of electron transfer to better understand substrate chemical reactivity and topography.

PHOTOSYSTEM I (PSI)

Photosystem I (PSI) is a protein complex present in most oxygenic photosynthetic organisms that has been optimized through natural selection to convert solar energy to electrical energy with high efficiency. The overall function is to harvest photons and utilize this energy to accomplish electron transfer (ET) through a series of redox centers.[2] The protein complex is about 500 kDa, with an 80 nm^2 footprint.[3] In nature, antenna pigments absorb the incident photons, which are then transported from antenna chlorophylls to the P_{700} reaction center. P_{700} is a chlorophyll dimer that accepts photons and energizes electrons resulting in a charge separation (Figure **1**).[4] The electrons generated here will travel through an electron transfer chain. The end of this chain is an Fe-S cluster denoted as F_B which reduces ferredoxin, and the reduced ferredoxin will subsequently provide electrons in a variety of crucial redox reactions in plants.[2]

The first investigation of PSI for alternative energy studies was performed by Greenbaum in 1985.[5] In this report, platinized chloroplasts were utilized for hydrogen production under photosynthetic conditions. They also showed that ET occurs across the interface between PSI and the platinum catalyst. Following this breakthrough, Greenbaum and co-workers utilized the photodiode property of PSI to study molecular electronics. In their study, they reported a method to control PSI adsorption and orientation by varying the head group of self-assembled monolayers (SAMs) on flat gold surface. They also measured the electrostatic potentials of PSI with Kelvin force probe microscopy (KPFM).[6]

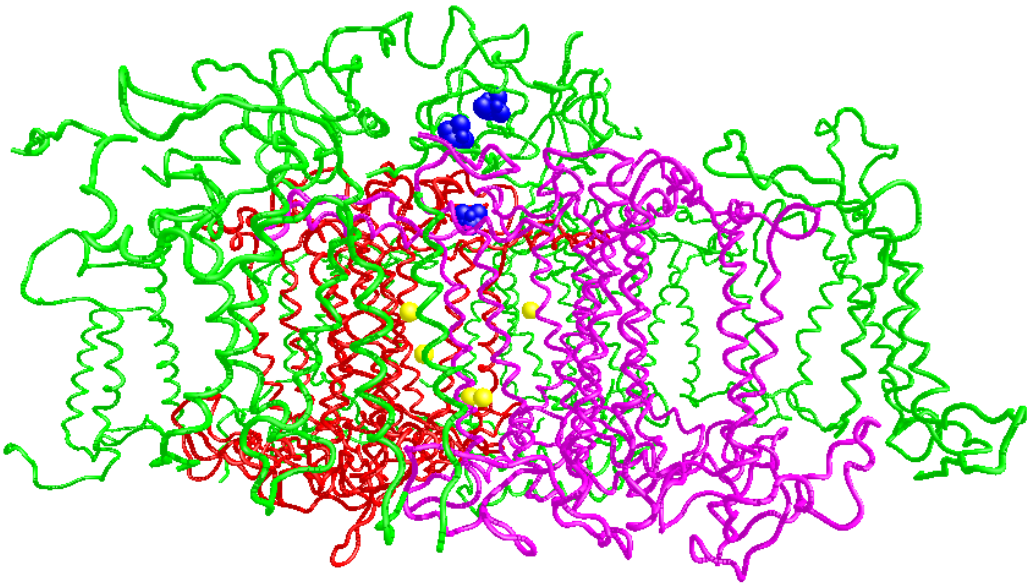

Figure 1. Structure Model of Plant Photosystem I. The positions of P700 reaction centers are shown in yellow; iron-sulfur complexes are highlighted in blue as ball structure; chlorophyll A is in red and chlorophyll B in purple; other subunits are in green. Atomic coordinates for the representations of PSI complexes used in this figure were contributed by Amunts *et. al.*[3] PDB ID 3LW5.

Additional groups are exploring fabrication of biohybrid devices with PSI. Baldo and coworkers integrated PSI complexes into a solid-state photovoltaic cell which showed internal quantum efficiencies of approximately 12%.[7] Terasaki's group has used PSI to fabricate photoelectrochemical cells and transistors.[8,9] Carmelli *et. al.* assembled photovatalic devices and examined the potential of a PSI monolayer on gold with KPFM and surface photovoltage spectroscopy (SPS).[10] They also investigated immobilized gene mutated PSI on gold and carbon nanotubes.[11]

Furthermore, some groups investigated the ET of PSI. Proux-Delrouyre *et al.* studied the electron transfer between cytochrome C6 and the P_{700} site, as well as between methyl viologen and the F_A/F_B site in solution.[12] The Rusling group tested reversible ET between electrodes and spinach PSI contained in thick, micron-scale lipid films; by selective removal of cofactors. They assigned the reversible peaks to the cofactors phylloquinone A1 and the ion sulfur clusters F_A/F_B.[13] From these

advanced studies, our group has looked into various ways of PSI immobilization methods, and studied the photo-electrochemical properties.

Our group has previously immobilized spinach-extracted PSI to metal surfaces and studied interfacial electrochemistry. Samuel Ko *et.al.* utilized ω-terminated alkanethiol SAMs to modify gold and deposited Triton X-100 stabilized PSI onto the surface. They also determined that PSI adsorbs onto high-energy surfaces such as -OH and -CO_2H terminated alkanethiols but does not adsorb to low-energy surfaces such as CH_3-terminated groups under their conditions.[14] Dr. Madalina Ciobanu characterized PSI on patterned surfaces with distinct regions of -CH_3 and -OH terminated SAMs on gold by SECM.[15] In her study, she demonstrated that the SECM results correlated with Samuel Ko's conclusion and proved that PSI did absorb onto -OH, and not on -CH_3.

Ciobanu also achieved reversible direct ET between the gold electrode and the P_{700} reaction center of a PSI monolayer adsorbed onto a hydroxyl-terminated hexanethiol modified gold electrode. This study demonstrated the success of molecular wiring from gold to PSI.[16] Dr. Chris Faulkner reduced the time required for PSI attachment onto the SAMs modified gold by ~80 fold compared to PSI adsorption from solution by applying vacuum-assisted assembly. This method also resulted in increased photocurrents due to the increased thickness of the PSI film.[17]

Dr. Peter Ciesielski enhanced the photocurrent by four times with the employment of nanoporous gold leaf, which greatly improved PSI/electrode interfacial area.[17] With the development of a biohybrid photoelectrochemical cell, the photocurrent was improved another five times.[18] By applying multilayer films of PSI with vacuum- assistant method, photocurrent was again improved five times.[19] All the photocurrent production capability increased while increases with PSI film thickness.

Previous work by our group and others have substantially increased our knowledge of PSI. However, these studies only offered information about the PSI/electrode interface, or the PSI electrochemical properties in solution. Further understanding of the redox processes occurring at the two docking sites of PSI could help to better manipulate PSI into biofuel cells or eventual carbon fixation or hydrogen production applications. In these studies, SECM was applied to monitor both sides simultaneously. In addition, redox mediators were screened to facilitate multilayer PSI photocurrent production.

Chapter IV investigates the electrochemical behavior of PSI with SECM. PSI acts as a natural photodiode and has two redox docking sites whose electron transfer process occurs in sequence. SECM was employed to monitor both redox sites of PSI simultaneously. The first amperometric photocatalytic response at both the substrate and the tip electrodes over PSI is collected, and the measurement suggested that electron transfer can be controlled by the potential setup at electrodes. Furthermore, approach curves elucidated electron transfer in multilayer PSI.

Chapter V discusses the electrocatalytic activity of photoreductive platinum on a PSI multilayer. In this study, multilayer PSI films were immobilized on solid substrates, and were utilized to photoreduce platinum particles onto the substrate from platinum salts in solution. The platinum particles were characterized by scanning electron microscope (SEM) and confirmed by energy dispersive x-ray spectroscopy (EDX). SECM was used to electrochemically image individual platinum particles immobilized on the substrate, and investigate the catalytic activity of platinum for hydrogen production.

REDOX MEDIATOR

As described in the previous section, in nature, following the irradiation of PSI in green plants, the $P700^+$ is reduced by plastocyanin while ferredoxin accepts the electron from F_B^-, preparing PSI to facilitate ET again upon photon capture. Unfortunately, plastocyanin and ferredoxin are difficult to isolate and cannot be regenerated in a simple artificial system. Thus, freely diffusing redox mediators have commonly been employed.[12, 13, 16, 17, 20]

Szentrimay et al. has reviewed mediators in 1977, and suggested that the properties for an "ideal" mediator in biological system include: (1) well-defined electron stoichiometry; (2) known formal potential ($E^{0'}$); (3) fast heterogeneous and homogeneous ET; (4) readily soluble in aqueous mediator at neutral pH; (5) stability in both oxidized and reduced forms; (6) no optical interference where optical monitoring of the biocomponent is used; and (7) no interaction with the biocomponent in a manner which alters its redox potential.[21] Fults et al. found a compilation for mediator compounds for the electrochemical study of biological redox systems in 1982. They indicate that the mediator structure and $E^{0'}$ are important parameters to consider.[22] The structure of the mostly extensive used mediators in this thesis is shown here (Figure 2).

Methyl Viologen (MV):

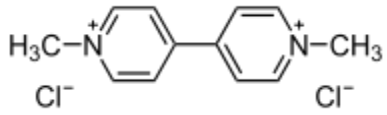

Ferrocenylmethyl-trimethylammonium hexaflorophosphate (FcTMA):

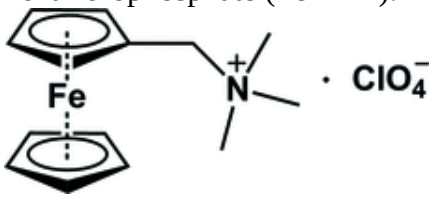

Riboflavin

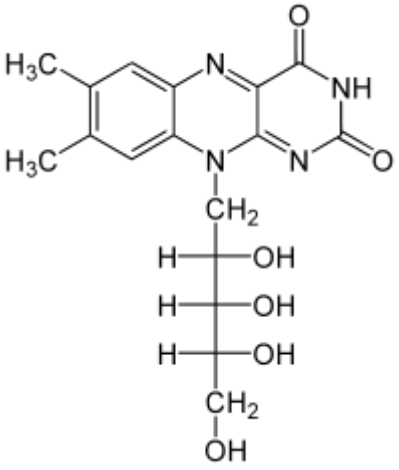

Figure 2**.** Structure of common mediators used in the thesis.

Chapter III evaluates redox mediators for a PSI-based electrode system. The indirect electron transfer properties of various mediators with PSI modified electrodes were investigated. The study was undertaken to determine how these mediators impact the photocurrent. This work has demonstrated that the choice of redox mediator has a profound influence on the photocurrent produced by the PSI modified gold electrodes, in which mediators with more positive formal potentials produced larger photocurrents.

SHEWANELLA

The genus *Shewanella* is a subset of Geobacter, found in a wide range of environments. *Shewanella oneidensis* was named after Oneida lake, NY, USA, where the species and strain had been isolated from sediments.[23] The different strains were named MR-1, MR-2, MR-3 and MR-4 by Stenstrom and Molin in 1990.[24] The *S. oneidensis* MR-1 is the species studied herein. This species was noted as a gram negative gamma proteobacteria, has cellular dimensions of 2-3 μm in length and 0.4-0.7 μm in diameter.[25] It was isolated in 1987 with the ability to couple the oxidation of organic carbon in the reduction of insoluble manganese (IV).[26] The fact that many oxidized forms of heavy metals are capable of being reduced by microbes, thereby relieving toxicity, is also a driving force to study dissimilatory metal reducing bacteria (DMRB). DMRB studies have opened the door for removing the toxic form of heavy metals from ground water where they pose dangers to human health.[27, 28] *S. oneidensis* MR-1 is known to be capable of the bioremediation of heavy metals, as well as the electrical reduction of an anode in microbial fuel cell devices, making it a prime candidate for practical use.[25]

When *Shewanella* show their ability to reduce Fe (III) oxide, which was precipitated in either alginate beads or nano-porous glass beads in two separate studies, it was discovered that a soluble

shuttle or chelator must be involved in the extracellular ET process.[29, 30] Marsili and coworkers observed that the *Shewanella* generated current decreased dramatically when the surrounding medium was exchanged with fresh medium. However, if the original medium was put back after centrifugation to remove planktonic cells, the original level of current immediately returned. In addition, they were able to identify the soluble mediator as riboflavin by mass spectrometry.[31] Jiang et al. fabricated an insulator layer over nanoelectrodes to control access of bacteria to the electrode surface, and the current produced by *S. oneidensis* was similar, regardless of the electrode configuration. The ability to reduce an electrode without direct contact suggests that the extracellular respiratory ET process is a shuttle mediator.[32]

Shewanella are able to generate energy with various potential electron acceptors, which has drawn research interest in environmental studies.[23] Understanding of the behavior of *Shewanella* species on electrodes could facilitate the development of electrochemical systems that incorporate whole cells as miniature bio-refineries, acting to couple the flow of electrical current into cells with the production of a desired metabolite. Applications of *Shewanella* include bioremediation, bioenergy-microbial fuel cells, and synthetic biology.[33]

Chapter VI detects the dissimilatory metal reduction pathways of *Shewanella* with spatial resolution. *Shewanella oneidensis* bacteria were able to utilize insoluble metals as respiratory substrates. Since insoluble substrates cannot freely diffuse into the cell, *Shewanella* must exhibit a capability of transferring electrons between the cellular interior and the insoluble substrates. The pathways for electron flow are known as dissimilatory metal reduction (DMR) pathways, which include direct and indirect pathways. Direct *in situ* detection of current through specific DMR pathways is a challenge for conventional analytical instruments. Here, SECM was used to detect the

direct and the indirect DMR pathways. Additionally, SECM substrate generation / tip collection mode were used to monitor the cellular viability and flavin concentration. The results will amplify our understanding of distinguishing between the DMR pathways and the function of flavin in these pathways. This understanding will facilitate the optimization and utilization of *Shewannella sp.* for bioenergy, electrosynthesis, and bioremediation applications.

By investigation of the multilayer PSI system with electrochemical methods, we found that the ET in PSI can be further improved by the selection of proper redox mediators, as well as the application of electrode potentials. In addition, the photoreduction ability of PSI can be used to precipitate platinum for hydrogen production. SECM is a powerful tool for ET detection. Additionally, further studies with the SECM show that *Shewanella* biofilms are able to secrete riboflavin which acts as an electron shuttle to facilitate extracellular ET. We hope our studies with PSI and *Shewanella* will provide insight for novel platforms for bio-hybrid devices and alleviate growing energy demand and environmental pollution.

CHAPTER II

EXPERIMENTAL INSTRUMENT AND ANALYTICAL METHODS

The studies presented in this dissertation are predominentely electrochemical analytical methods. However, scanning electron microscopy and UV-Vis spectroscopy were also employed to provide elucidate additional information about the system under study. Detailed descriptions about the parameters of each method employed in the experiments are provided in each subsequent chapter, while this chapter offers the general background and theory facilitating the interpretation of relevant results and conclusion.

PREPARATION OF ELECTRODES

For PSI experiments, the substrate electrode was either a 2 mm diameter gold disk electrode (CH Instrument, Inc.) or a gold wafer. These electrodes may further modified by SAMs and PSI. For *Shewanella* experiments, the biofilm was cultured on a 3 mm diameter glassy carbon electrode (CH Instrument, Inc.). Before each experiment, the substrate electrodes are polished with 0.25 μm diamond polish (Buehler) and 0.05 μm alumina. All gold electrodes were modified with SAMs before modification with PSI.

Ultramicroelectrode (UME, diameter $\leq$ 25 μm) is used in SECM as the second working electrode (WE). The UME used in Chapter IV were fabricated by sealing a 10 μm diameter gold wire (Goodfellow) into Pyrex glass tubes according Bard *et. al.*[34] The UME used in Chapter VI was fabricated with a 7 μm diameter carbon fiber according to the similar process. A 2 μm diameter platinum UME (CH Instrument, Inc.) was used for the PSI-Pt image experiment in Chapter V. Before each experiment, the UMEs were polished by Buehler grand paper, and 0.05 μm alumina to

form a smooth surface and maintain a RG ratio of 2-5. Metal UMEs and the 2 mm Au disk substrate electrode were acid cleaned in a 0.5 M H_2SO_4 solution following the polishing step. The performance of UME was checked in cyclic voltommetry with the tip far away from the substrate (in bulk solution). The voltammogram should be well shaped with a flat plateau (steady-state current) and little hysteresis (Figure 3).

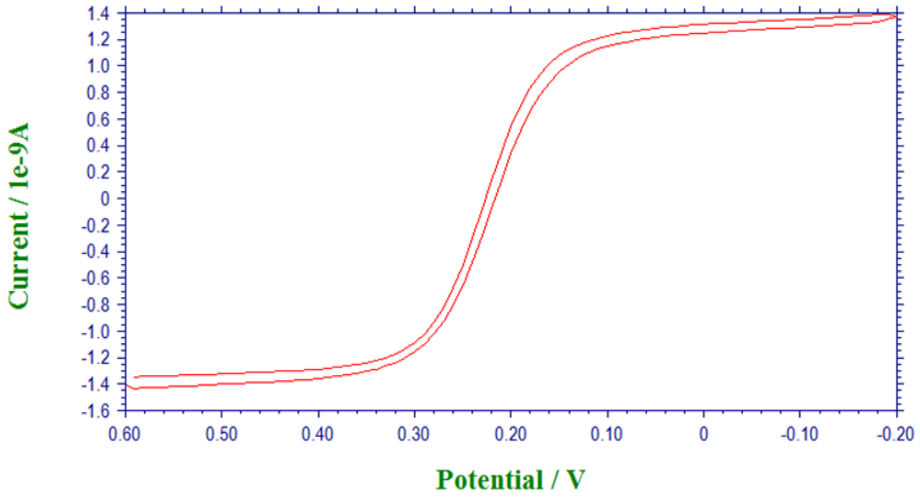

Figure 3. Typical UME cyclic voltammogram.

The reference electrode was an aqueous Ag/AgCl (3 M KCl) from CH Instruments, Inc. The counter electrode was either a platinum wire in SECM experiments or platinum mesh in traditional electrochemical experiments, respectively.

PSI EXTRACTION

PSI complexes were extracted from baby spinach as described previously.[16,19, 35, 36, 37] Briefly, thylakoid membranes were isolated via maceration followed by centrifugation using the method of Reeves *et al.*[36] coupled with several adaptations made by Ciobanu.[16] Secondly, PSI complexes were separated from the thylakoid membranes by additional centrifugation followed by purification using a chromatographic column packed with hydroxylapatite.[35, 37] Aliquots of 1 mL of the column

effluent were then dialyzed in deionized water for 24 h using 10,000 MW cut-off dialysis tubing (Spectrapore), which reduced the initial concentrations of Triton X-100 (0.5 g L^{-1}), Na_2HPO_4 (0.2 M), and NaH_2PO_4 (0.2 M) to 0.25 mg L^{-1} , 0.1 mM, and 0.1 mM, respectively, assuming complete dialysis. The total chlorophyll concentration of the product was determined by the method of Porra *et. al.*[38] and the P_{700} concentration was determined using the method of Baba *et. al.*[37] The suspended PSI elution buffer was aliquoted into each 2 mL bullet tubes to store at -80 ℃, and thaw to room temperature before use.

ANALYTICAL ELECTROCHEMISTRY

Cyclic voltammetry (CV) and photochronoamperometry are electrochemical methods that have been carried out in most of experiments in this work, including both traditional electrochemical systems, and SECM. The electrochemical behavior of microelectrodes is distinct from macroelectrodes due to the smaller size and less electrical resistance of UME, and will be discussed in detail in the SECM section.

Cyclic Voltammetry

Cyclic voltammetry (CV) is a popular technique in electrochemical studies for novel systems because of its ability to obtain information including redox system reversibility, electron transfter (ET) kinetics, and absorption properties onto electrodes. CV is a potential sweep method in which the current is recorded while the electrode potential is changed linearly with time between two values, an initial potential E_i and a final potential E_f, with the potentials will be inverted in the second sweep. If the formal potential ($E^{0'}$) of redox mediators are in the range of E_i *to* E_f, then peaks due to increased flow of current in the measurement can be observed. When the working electrode potential (E_W) approaches the $E^{0'}$, there is an increase of ET rate between electrode and redox

couple because the energy barrier between them is decreasing. When $E_W > E^{0'}$, the reaction rate will continue increasing until the reaction becomes diffusion-limited, and a peak in current will appear due to the depletion of reactant in the region close to the electrode. The typical voltammogram has been illustrated in Figure **4**.

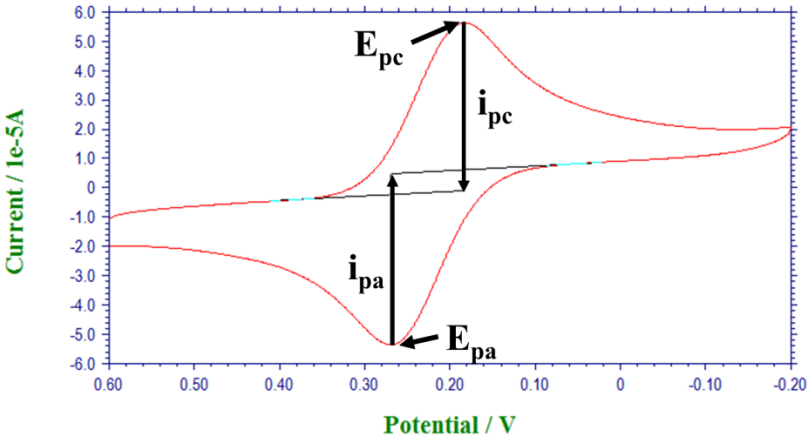

Figure 4. Typical cyclic voltammogram, where i_{pc} and i_{pa} show the peak cathodic and anodic current of a reversible reaction, respectively.

Standard potential (E^0) is the critical potential at which the redox processes occur at standard conditions, and it is a characteristic property for redox mediators. E^0 is always replaced by $E^{0'}$, which accounts for the solution and electrode conditions. The value of $E^{0'}$ for each mediator can be determined as the average of the anodic ($E_{p,a}$) and cathodic ($E_{p,a}$) peak potentials from the resulting cyclic voltammetry.

One of the key features of the cyclic voltammogram is the peak height. According to Randles-Sevcik equation:

$$i_p = \left(2.69\times10^5\right) n^{3/2} A D_0^{1/2} C_0^{*} \nu^{1/2} \qquad (1)$$

where n is the number of electrons transferred, v is the scan rate, D_O is the diffusion coefficient, and C^* is the redox couple bulk concentration. This equation can be used to calculate the variables.

CV can also be used to diagnose whether a system is reversible according to the following criteria:

$$i_p \propto v^{1/2} \tag{2}$$

$$\Delta E_p = E_{pa} - E_{pc} = \frac{59}{n}\, mV \; at \; 298K \tag{3}$$

$$\left| \frac{i_{pa}}{i_{pc}} \right| = 1 \tag{4}$$

Photochronoamperometry

Photochronoamperometry is one of the most frequently used electrochemical analytical techniques that have been applied in the photocurrent studies. It is a derivation of chronoamperometry, is a measurement of current - time behaviour while a potential step is applied to the working electrode in the presence of redox mediators.[39] In the photochronoamperometric measurements, a constant potential was applied, and the light exposure is used to replace the potential step in chronoamperometry. If the target electrochemical system contains components that are sensitive to the light irradiation, the difference in the measured current will demonstrate the effect of the illumination.

For a one electron diffusion-controlled reversible redox couple system, the net current produced on the electrode surface at time *t* is:

$$i_{net}(t) = FA\left[k_{red} C_0(0,t) - k_{ox} C_R(0,t) \right] \tag{5}$$

where *F* is the Faraday constant, *A* is the area of the electrode, $C_O(0,t)$ and $C_R(0,t)$ are the respective concentrations of the oxidized and reduced form of the redox couple at the electrode surface, and k_{red} and k_{ox} are the heterogeneous rate constants for the reduction and oxidation reactions, respectively.

In order to minimize the net current while studying photocurrent production, the open circuit potential (E_{eq}) of the PSI-modified electrodes in dark conditions is determined first and then applied on the WE to obtain a zero net current. However, in order to further study the electron transfer direction in PSI films, an overpotential (η) is also applied in certain experiments. η is the extent to which the reaction is driven beyond the equilibrium potential,

$$\eta = E_W - E_{eq} \tag{6}$$

E_W is the potential applied to the WE. η can be either positive or negative.[40] The negative η motivates the heterogeneous reduction of the redox couple, and generates cathodic current, reported in positive direction by convention, while positive η generates anodic current in the negative direction. The typical figure is shown in Figure **7** in Chapter III.

The traditional electrochemical experiments were mainly presented in Chapter III. A homemade three-electrode cell using the PSI-modified gold electrode as the WE, the Ag/AgCl as reference electrode, and the platinum mesh as counter electrode has been employed in the experiments. All experiments were performed on a CHI 660a electrochemical workstation equipped with a Faraday cage. The experiment presented in Chapter IV, V, and VI were performed in a four- electrode system with a second WE using UME in the SECM platform (CHI 900).

Scanning Electrochemical Microscopy (SECM)

SECM is a powerful tool for studying structures and processes in micrometer and submicrometer sized systems.[41] The development of SECM has taken advantage of improvements of ultramicroelectrodes (UMEs) and scanning tunneling microscopy (STM).[34] By scanning or approaching the tip of the UME on/to a substrate, chemical changes can be introduced and electrochemical perturbations can be analyzed.[41] UMEs with varied size, shape, and composition

have been fabricated; however, a disk-shaped UME is preferred over other shapes due to its easy characterization, thus only disk UMEs will be discussed here. The typical diameter of a UME is smaller than 25 μm where measured current is relatively steady, and limited by mass-transfer:

$$i_{t,\infty} = 4nFDca \quad (7)$$

Where F is the Faraday constant, D is the diffusion coefficient, c is the concentration, and a is the radius. Other factor that affects the current is the radius of the insulating sheath, r_g. The ratio of r_g and a is defined as RG.[34] The tip current, i_t, is affected by electrochemical reactions at the tip electrode, the sample substrate, and the tip to substrate distance, d, and the conductivity of the sample substrate. Several operation modes have been employed in the current work; these include feedback mode, generation / collection mode, and constant height image mode.

In the feedback mode, the tip is typically immersed in a redox mediator solution (*e.g.*, a reducible species, O), which may also contain supporting electrolyte. When the tip potential is negative enough to reduce the oxidant, the following reaction occurs: $O + ne^- \rightarrow R$

If the tip is far from the surface of substrate, the current is governed by diffusion of O to the UME, and will get to the limiting current, $i_{t,\infty}$ (Figure **5**a). When the tip moves to within a few tip radii of the substrate, if the substrate is an insulator the diffusion of oxidant is blocked by the substrate. Moving the tip close to the insulator lowers i_t and generates negative feedback (Figure **5**b). If the tip is brought close to a conductive substrate, the reduced formed diffuses to the substrate, and can be oxidized back to O: $R \longrightarrow O + ne^-$. This process produces extra O at the tip, and the obtained i_t is larger than $i_{t,\infty}$ (positive feedback, Figure **5**c).[42] In the feedback mode, i_T and the tip position were recorded as the tip was scanned in a direction perpendicular (z-direction) or horizontal (x, y-direction) to the substrate surface. The distance scale was made dimensionless by dividing the tip electrode radius. The experimental feedback current was normalized by dividing by $i_{t,\infty}$. For

approach curve measurements, the tip was positioned directly above the sites of interest. Measurement of i_t provides information about the topography and electrical and chemical properties of the PSI modified substrate in Chapter IV, and the flavin concentration profile produced by *Shewanella* biofilm in Chapter VI.

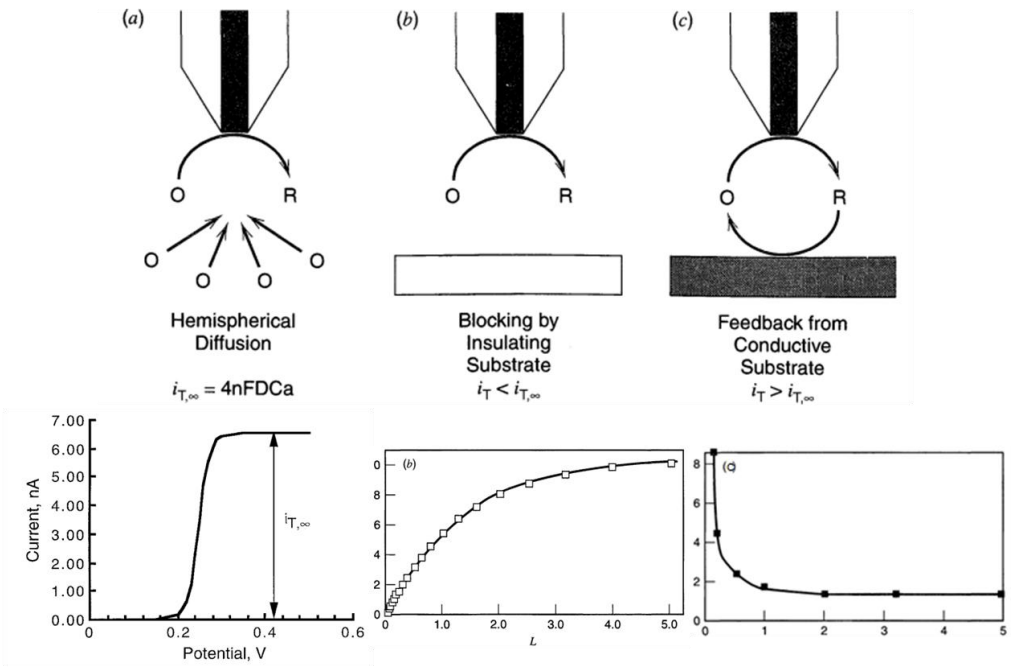

Figure 5. Schematic illustration of SECM feedback Mode and theoretical approach curves. Top: (a) The UME tip is far from the substrate, and a typical steady-state voltammogram. (b) Tip is close to an insulating substrate, and its corresponding negative feedback AC. (c) Tip is close to a conductive substrate, the positive feedback AC is shown beneath it.[1]

Collection / generation mode can offer spatial composition information, and includes two different types, schematic demonstration is in Figure **6**.

Tip Generation / Substrate Collection (TG/SC) mode is similar to feedback mode in that both an electroactive species is generated at the tip and collected at the substrate. A TG/SC experiment includes simultaneous measurements of both tip and substrate currents (i_T and i_S).[34] For simple one-step heterogeneous electron transfer at steady state, $i_T / i_S > 0.99$ when the tip-substrate distance is

not larger than one tip radii. Under this condition, the tip generated species predominantly diffuses to the large substrate, instead of escaping from the tip-substrate gap (Figure **6**A).[41]

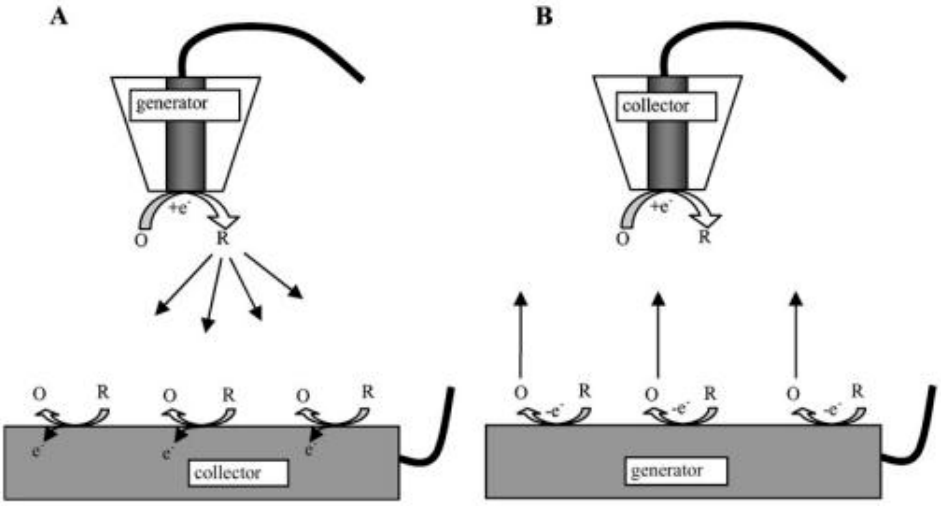

Figure 6. Schematic illustration of TG/SC mode (A) and SG/TC mode (B). A) The tip generates species R by reduction of O in solution; R diffuses toward the substrate and is reoxidized to O. (B) O is electrogenerated at the substrate surface and collected at the tip.[9]

Another generation / collection mode is Substrate Generation / Tip Collection (SG/TC). Usually, the substrate is much larger than the tip and generates a thicker diffusion layer than that at the tip. Ideally, the tip will not perturb the concentration profile during the test. However, this is very difficult due to: (1) the moving of tip stirs the substrate diffusion layer (2) when the substrate is large, no true steady state can be achieved and (3) the tip blocks the diffusion to the substrate surface. In addition, the collection efficiency (i_S / i_T) in SG/TC mode is much lower than that in the TG/SC mode (Figure **6**B).[41]

A SECM image can be obtained by scanning the tip in the x-y plane and simultaneously monitoring the tip and substrate current. Since the tip is maintained in the same distance between tip and substrate, it is called constant height mode. The image can be presented in color coded plot or 3-D surface plot, and offer information about substrate topography and conductivity as a function of

tip position. The resolution is dependent on tip diameter and tip-substance distance.[40] Constant height image mode was used to map the hot spots of platinized PSI substrate that can produce hydrogen in Chapter V. Both in generation/collection mode and in the image operation mode, an approach curve was first performed to position the tip 1 - 2 tip radius distances from the substrate. At this distance, reasonable resolution images can be achieved.

The SECM experiments were performed with a CHI900 (CH Instrument, Inc.). The UME was firmly placed on a three-axis stage with piezoelectric inchworms, and controlled by the CHI 900 controller. The substrate holder for SECM was a Teflon cap with screw holes. The cell was set up with the tip directly above the substrate electrode. The potentials of tip and substrate were controlled by a bipotentiostat.

Scanning Electron Microscopy (SEM)/ Energy Dispersive X-ray spectroscopy (EDX)

Scanning Electron Microscopy (SEM) applies a focused beam of electrons on the surface of the interested sample. The electrons interact with electrons in the sample, producing secondary electrons or back-scattered electrons which offer information about the sample's surface topography and composition. The electron beam is generally scanned in a raster scan pattern, and the position of the beam can be combined with the detected signal to produce an image. SEM can achieve resolution of a few nanometers.[43] A more advanced function of SEM is to integrate with Energy Dispersive X-ray spectroscopy (EDX). EDX is an analytical technique used for the elemental analysis or chemical characterization of a sample. It relies on the investigation of an interaction of some source of X-ray excitation and a sample. Its characterization capability is due to

the unique atomic structure of each element, allowing unique set of peaks on its X-ray spectrum. By combining SEM and EDX, the composition on a substrate surface is easily characterized.

The combination of SEM and EDX has been applied in Chapter V to confirm the photo-reduction of platinum by PSI. The SEM experiments were performed on a Hitachi S-4200 instrument. SEM images were collected with an accelerating voltage of 20 kV. EDX analyses were performed using an accelerating voltage of 20 kV and an emission current of 20 μA.

Ultraviolet-visible (UV-Vis) Spectroscopy

Ultraviolet-visible spectroscopy (UV-Vis) uses light in the visible and adjacent (near-UV and near-infrared) ranges. The absorption or reflectance in the visible range can promote electrons in molecular or atomic orbitals of the material to excited states. For each specific molecule, the energy required to initiate the electronic transition is specific. UV-Vis spectroscopy is a commonly used analytical instrument for quantitative and qualitative determination.[44] According to the Beer-Lambert Law, absorbance (A) is proportional to the concentration of the absorbing species (c) and the path length (b).

$$A = \varepsilon bc \tag{8}$$

where ε is the extinction coefficient. This law has been used to determine the concentration of PSI suspended in the elution solution after extraction.

The wavelengths of absorption peaks can be correlated with the types of bonds in a given molecule and are valuable in determining the functional groups within a molecule. This feature of UV-Vis has been employed in Chapter III to compare the UV-vis absorption between PSI and redox mediators. The spectra were collected by a Cary 100 Bio UV-Visible Spectrophotometer dual beam UV-Vis from 350 to 750 nm of the PSI and mediators in phosphate buffer.

Optical Microscopy

Optical microscopy is a classical method for obtaining detailed information about the physical nature of surfaces that are beyond the resolution of human eye (about 100 μm). It can be considered as an extension of our eyes, which determines the shape and size of small objects uses visible wavelength light.[43] The resolution (r) of light microscope is limited by the wavelength of light used, and the numerical aperture (NA) of the system:

$$r = \lambda / 2NA \tag{9}$$

where λ is the wavelength of light used, and NA of OLYMPUS BX41 is from 1.1- 0.16. If λ is taken to be 0.55 μm when used white light, the resolution of the OLYMPUS BX41 microscope would be 0.25- 1.72 μm. OLYMPUS BX41 microscope has been used in checking of UMEs fabrication and electrode polishing situation. It has also been used to observe assembled PSI substrate in Chapter IV.

CHAPTER III

EFFECT OF REDOX MEDIATOR ON THE PHOTO-INDUCED CURRENT OF A PHOTOSYSTEM I MODIFIED ELECTRODE

Photosystem I (PSI) is a protein complex located within the thylakoid membrane of green plants and cyanobacteria.[3] It has drawn the attention of researchers due to both its ability to convert absorbed solar energy into a charge separation with near-unity quantum efficiency and its inspiration for biomimetic alternative energy approaches. The key questions in utilizing this protein complex in power conversion devices include how to immobilize it onto electrodes while maintaining functionality and how to get the optimal electron transfer (ET) from the active site of PSI after photo-induced charge separation.[20] PSI monolayer and multilayer films have been immobilized on various electrode substrates through self-assembly or genetic modification, and their photo-activity has been demonstrated using a variety of techniques.[7, 11, 16, 17, 45]

Photocurrent is an important parameter for the evaluation of whether the PSI reaction centers are used effectively in the artificial environment. However, since the active sites of PSI are buried deep in the protein, the ET rate is significantly decreased, and the direct electron transfer (DET) between PSI and the electrode surface is not favorable. Our groups' first attempt to interface PSI with a gold electrode modified with a self-assembled monolayer (SAM) generated a weak photocurrent in the range of 3 nA cm^{-2}.[16] Because ET in PSI occurs in less 1 μs, photocurrent densities near 1 mA cm^{-2} should be expected, assuming an immobilized monolayer of PSI with 0.5 pM cm^{-2} coverage.[46, 47] By optimizing the electrochemical conditions, we may begin to approach the theoretical photocurrent densities of these systems.

In nature, when PSI in green plants is irradiated, an electron in the P700 reaction center is excited, which then travels down an ET chain to a terminal iron-sulfur cluster (denoted as F_B). Following excitation, the $P700^+$ is reduced by plastocyanin while ferredoxin accepts the electron from F_B^-, preparing PSI to facilitate ET again upon photon capture. Unfortunately, plastocyanin and ferredoxin are difficult to isolate and cannot be regenerated in a simple artificial system. Thus, freely diffusing redox mediators have commonly been employed.[12, 13, 16, 17, 20]

Several methods have been utilized to enhance the photocurrent of PSI modified electrodes. These include increasing the surface area of the electrode by nanoporous gold leaf films,[48] increasing layers of PSI,[17, 19] attempts to wire the reaction centers with gold nanoparticles or other molecular wires,[8] and wiring PSI with solid supports such as photoprecipitated metal colloids and redox polymers.[49, 50] In all of these attempts, redox mediators were employed as electron donors or electron acceptors. Previous work in our group has demonstrated that the choice of mediator has a significant effect on the resulting photocurrent from the biohybrid device.[51] However, there has been no systematic study that compares the mediators in the same environment to offer insights for future application.

Here we investigate how simple and commonly used mediators impact the photocurrent of PSI immobilized on the surface of an electrode. In these experiments, PSI extracted from spinach was deposited onto gold electrodes. The chosen redox mediators have formal potentials that span the two ET sites of PSI: P700 (E_{P700} = +0.31 V vs. Ag/AgCl) and F_B ($E_{FA/FB}$ = -0.58 V vs. Ag/AgCl). [16] These redox mediators include inorganic complexes, organic compounds, and biological mediators (Table 1). Additionally, combinations of different mediators were examined to investigate possible

synergistic effects. Our work reveals several factors that are important to the performance of photoelectrochemical cells and offers a simple method for screening mediators.

Table 1. Redox mediators and their properties listed in order of $E^{0'}$

Redox Mediators	Abbreviations	ET Property	$E^{0'}$ / V (vs. Ag/AgCl)[a]	Mediator Solution Color
Ferredoxin	Ferredoxin	e^- Acceptor	-0.70	--
Methyl Viologen	MV^{2+}	e^- Acceptor	-0.65	Clear
Anthraquinone-2-sulfonate	AQS	e^- Acceptor	-0.45	Clear
2-Hydroxy-1,4-naphathoquinone	HNQ	e^- Acceptor	-0.268	Light orange
Methylene Blue	MB	e^- Acceptor	-0.2	Dark blue
Hexaammineruthenium (III)	$Ru(NH_3)_6^{3+}$	e^- Acceptor	-0.11	Clear
2,6-dichloroindophenol	DCPIP	e^- Acceptor	0.09	Dark Blue
Plastocyanin	Plastocyanin	e^- Donor	0.17	--
Ferricyanide	$Fe(CN)_6^{3-}$	e^- Acceptor	0.2	Light yellow
Ferrocyanide	$Fe(CN)_6^{4-}$	e^- Donor	0.2	Clear
Cytochrome C	Cyt C	e^- Acceptor	0.27	Red
Sodium Ascorbate	NaAsc	e^- Donor	0.31	Clear
Ferrocenylmethyl-trimethylammonium hexaflorophosphate	FcTMA	e^- Donor	0.44	Light yellow
Iodide/Triiodide	I^-/I^{3-}	--	0.48	Light brown

[a] This $E^{0'}$ is the experimental data based on the PSI modified electrode substrate

EXPERIMENTAL

Materials

The chemicals were purchased as follows: potassium chloride (KCl), and potassium ferricyanide ($K_3Fe(CN)_6$) from Fisher Scientific; methyl viologen (MV), 2-aminoethanethiol hydrochloride, sodium ascorbate (NaAsc), anthraquinone-2-sulfonate (AQS), and terephthalaldehyde (TPDA) from Aldrich Chemical; 2-hydroxy-1,4-maphathoquinoe (HQN), hexaammineruthenium (III) ($Ru(NH_3)_6Cl_3$), iodine, methylene blue (MB), potassium ferrocyanide ($K_4Fe(CN)_6$), and cytochrome C (Cyt C) from Sigma-Aldrich; and 2,6-dichloroindophenol (DCPIP) from Sigma Life Science;

ferrocenylmethyl-trimethylammonium hexaflorophosphate (FcTMA) was prepared according to the method of Mirkin and co-workers.[15, 52]

PSI Extraction and Purification

PSI complexes were extracted from baby spinach as described previously.[16, 19, 37] Briefly, thylakoid membranes were isolated via maceration followed by centrifugation using the method of Reeves *et al.*[36] coupled with several adaptations made by Ciobanu *et al.*[16] Second, PSI complexes were separated from the thylakoid membranes by additional centrifugation followed by purification using a chromatographic column packed with hydroxylapatite.[35, 37] Aliquots of 1 mL of the column eluent were then dialyzed in deionized water for 24 h using 10,000 MW cut-off dialysis tubing (Spectrapore), which reduced the initial concentrations of Triton X-100 (0.5 g L^{-1}), Na_2HPO_4 (0.2 M), and NaH_2PO_4 (0.2 M) to 0.25 mg L^{-1} , 0.1 mM, and 0.1 mM, respectively, assuming complete dialysis. The total chlorophyll concentration of the product was determined by the method of Porra *et al.*[38] to be 5.8×10^{-5} M with a Chl a/ Chl b ratio of 3.6, and the P700 concentration was determined using the method of Baba *el al.*[37] to be 1.8×10^{-6} M, yielding a Chl / P700 ratio of 32.

Preparation of PSI Modified Gold Substrate Electrode

Gold electrodes were cleaned with piranha solution (3:1 concentrated sulfuric acid: 30% hydrogen peroxide) prior to use, rinsed with distilled water and ethanol, and dried by N_2 (g). The clean gold electrode was then immersed in 1 mM 2-aminoethanethiol solution for 1 h, rinsed with ethanol, dried by N_2 (g), and immersed in 1 mM TPDA for another hour, and rinsed and dried again.

The PSI-substrate assembly followed an established procedure[17], where an aqueous solution of dialyzed PSI was pipetted on top of the TPDA-capped 2-aminoethanethiol SAM. The substrate was

then placed in a vacuum chamber, and the liquid in the PSI solution was evaporated with vacuum assistance.

Mediator Preparation

200 μM of each mediator solution was prepared in 5 mM phosphate buffer solution (PBS) and 100 mM KCl solution. The mediators were degassed with nitrogen for at least 30 min before each experiment. Mediators were prepared at 200 μM is to ensure that all mediators could be solubilized at this concentration, and thus are comparable with each other. Mixed mediator solutions were prepared with 100 μM of each mediator.

Photoelectrochemical Characterization

All electrochemical measurements were performed using a CHI 660a potentiostat (CH Instrument, Austin TX). The electrochemical cell is a home-made three electrode system, with the PSI modified gold electrode as the working electrode, Ag/AgCl as the reference electrode, and a platinum mesh as the counter electrode. The working electrode had an exposed surface area of 0.27 cm^{-2}. Photochronoamperometric data were collected at 0, +100 and -100 mV overpotentials. The light source was a Gebrauch KL 2500LCD lamp used without any light filters.

UV-Vis Spectrometry Characterization

The UV-Vis spectra were collected by a Cary 100 Bio UV-Visible Spectrophotometer dual beam UV-Vis from 350 to 750 nm of the PSI and mediators in phosphate buffer. Most mediators were used as the prepared solution. However, mediators such as MB, DCPIP and Cyt C, which have high absorbance coefficients, were diluted 50 times before absorbance measurements.

RESULTS AND DISCUSSION

Photochronoamperometry was applied to study the photoactivity of PSI as well as the interaction between PSI and redox mediators. In photochronoamperometry, a constant potential is applied to the working electrodes and the resulting current is measured as time progresses in dark and light conditions. Figure **7** is an example of the raw data that is observed at various overpotentials. As seen on the graph, the observed photocurrent is dependent on the overpotential applied during these experiments. The photocurrent density was calculated by the subtraction between light (20-50 s) and dark (0-20 s and 50-70 s) current density, which is defined as J/ (nA/cm^2). To eliminate the interference of potential bias, most experiments were performed at 0 mV overpotential, which means that the experiments were carried out at the open circuit potential of the modified electrodes. However, the effect of overpotential on the resulting photocurrent was also investigated in the following sections.

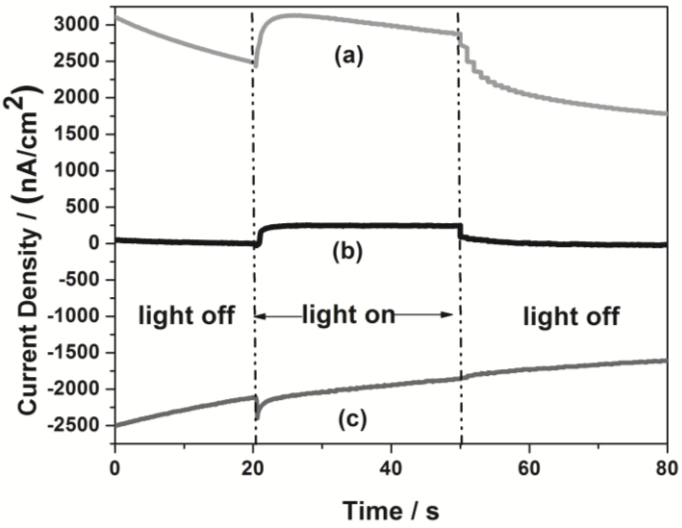

Figure 7. Raw data of photochronoamperometry performed on a PSI modified electrode using 200 μM DCPIP as the mediator. The curves represent measurements made at various potential bias: (a) -100 mV, (b) 0 mV and (c) 100 mV overpotential. Light was turned on from 20-50 s as indicated by the dashed lines.

Effect of Redox Mediator Formal Potential on the Photocurrent Density of PSI

To analyze the effect of formal potential on the resulting photocurrent, we used a 0 mV overpotential in this first set of experiments. The standard potential (E^0, at standard conditions) is the critical potential at which the redox processes occur, and E^0 is always replaced by formal Potential ($E^{0'}$) which includes the corrections for solution and electrode conditions, and is characteristic for each mediator.[39] There are several reasons to investigate the effects of the redox mediator $E^{0'}$ including: (1) it is unique for each redox mediator; (2) it shows the critical energy for mediators to transfer between oxidation states and interact with PSI cofactors; (3) it is a standard reference value to compare to E_{P700} and E_{FB}. The $E^{0'}$ for a reversible redox couple was determined as the average of the anodic and cathodic peak potentials from the resulting cyclic voltammetry of mediators on PSI-modified gold electrodes. For mediators whose reversibility could not be observed on a PSI modified electrode, the $E^{0'}$ values were extracted from the literature.

As seen in Table 1, the mediators investigated have $E^{0'}$ values which span the range of the reported redox potentials of F_B (-0.58 V vs. Ag/AgCl) and P700 (0.30 V vs. Ag/AgCl). Figure **8** shows that the photocurrent depends on the relative energy levels (redox potentials) of the PSI redox centers and the $E^{0'}$ of the solution species. For the PSI-modified gold electrode, there appears to be a trend favoring mediators with more positive $E^{0'}$ (lower energy). Discrepancies in this trend were observed with MB and DCPIP which may be caused by their high light absorbance in the visible spectrum, as described in the next section. The largest photocurrent density was observed by using $Fe(CN)_6^{3-}$, which had a photocurrent density close to 900 nA cm^{-2}. We also observed that metal-based mediators outperform organic compounds. This might be caused by the faster ET rate between metal based mediators and PSI cofactors than that between organic compounds and PSI.

Interestingly, these trends seem to be reversed when a p-doped silicon electrode is used, due to the differences between semiconducting and conducting electrodes.[53]

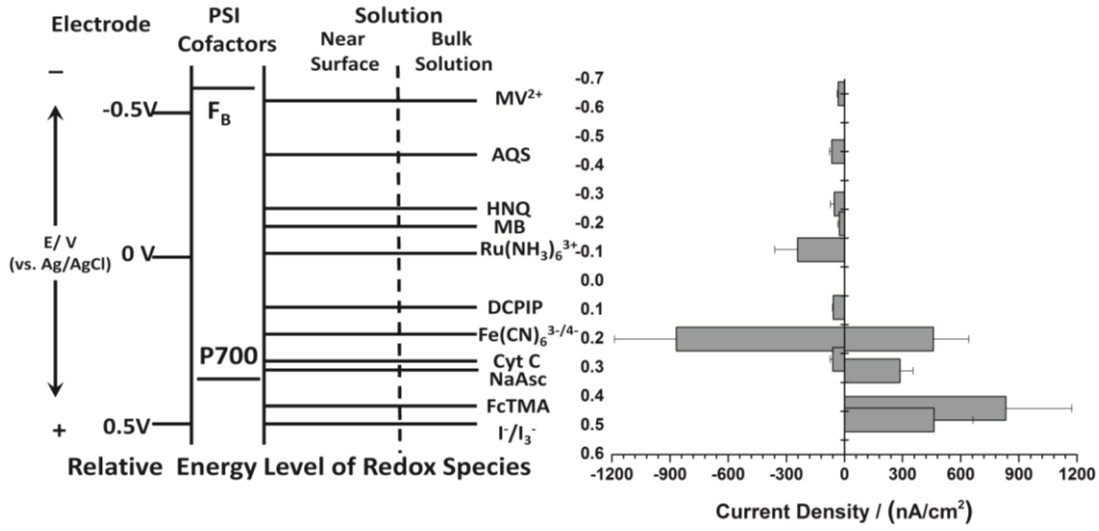

Figure 8. Energy level diagram of potentials of redox species in the PSI modified electrode chemical system, and photocurrent density of each corresponding mediator at 0 mV overpotential (n=3). The mediator concentration is 200 μM, prepared in PBS solution with 100 mM KCl.

Effect of Light Absorbance of Mediators on PSI Photocurrent Density

UV-Vis absorption spectrometry was employed to analyze the absorbance of each mediator solution from 350nm to 750nm compared to PSI (Figure **9**). Because light absorption in this range is responsible for charge separation in PSI, we hypothesized that mediators with absorbance that overlaps with the absorption peaks of PSI would hinder the observed photocurrent. As the black line in Figure **9** shows, the absorbance maxima of PSI appear at wavelengths that correspond to the Soret band in the blue region (300-450 nm) and the Qy transition band of chlorophyll a in the red region (650-750 nm).[54] Thus, any absorbance by the mediator in these regions would be expected to have a negative impact on the resulting photocurrent. As shown in Figure **9** and Table 1, the observed photocurrent for mediators with absorption overlap with PSI's Qy transition band (MB, DCPIP, and Cyt C) was significantly lower than expected. Interestingly, when the mediator's

absorbance overlaps with PSI's Soret band (FcTMA, ferricyanide, and ferrocyanide) the photocurrent seemed unaffected. One possible explanation is that the Soret band is not critical to the initial electronic transactions that feed excitation energy to P700, the primary reaction center of PSI. This would indicate that the Qy band is more important than Soret band for the photo-activity for PSI.

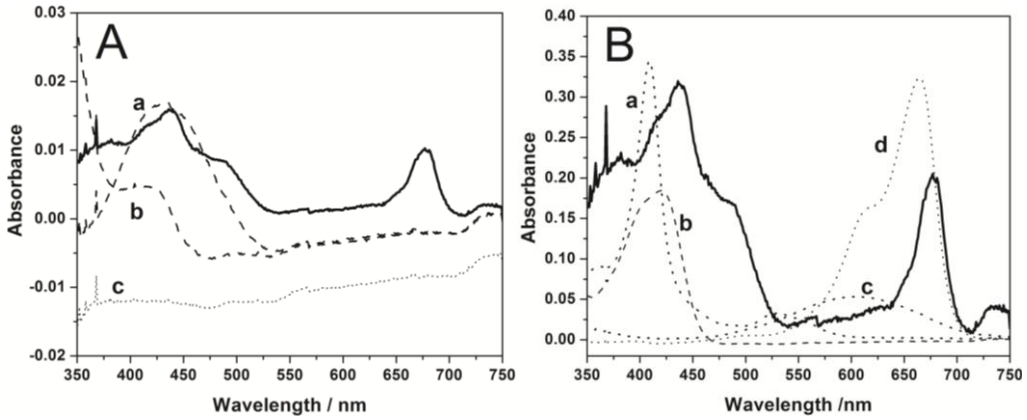

Figure 9. UV-Vis Spectra of redox mediators (dotted line) and PSI solution(continuous line). Redox mediators were prepared in 200 μM solutions as descibed in the experimental section. The PSI solution was prepared by diluting the dilalized solution by 50. (A) shows redox mediators with low absorbance (a) FcTMA, (b) $Fe(CN)_6^{4-}$, (c) PBS; while (B) show redox mediators with high absorbance. PSI absorbance data has been multiplied by 20, and redox mediator solution (a) Cyt C, (c) DCPIP and (d) MB has been dilluted 50 times, (b) $Fe(CN)_6^{3-}$ has not been diluted.

Effect of Overpotential on Photocurrent

In order to further elucidate the relationship between PSI and redox mediators for photocurrent production, photochronoamperometric experiments were performed at positive and negative 100 mV overpotentials. Overpotential (η) is the extent to which the reaction is driven beyond the equilibrium potential, $\eta=E-E_{eq}$; it can be either positive or negative.[40]

As shown in Figure **10**, overpotential nearly always enhances the observed photocurrent. In the case of +100 mV overpotential, the trend of photocurrent density is very similar with it at 0 mV: higher photocurrent density is observed for the mediators that have $E^{0'}$ closer to P700. Interestingly,

some mediators demonstrated significant photocurrent enhancement as a result of applying a negative overpotential. In the case of DCPIP, the photocurrent at -100 mV overpotential increased approximately 35 fold. Because the dark current significantly increases as well (Figure 7), we can assume that the mediator can be directly reduced or oxidized at the electrode as well. In the presence of light, the PSI further catalyzes the reaction to enhance the observed current.

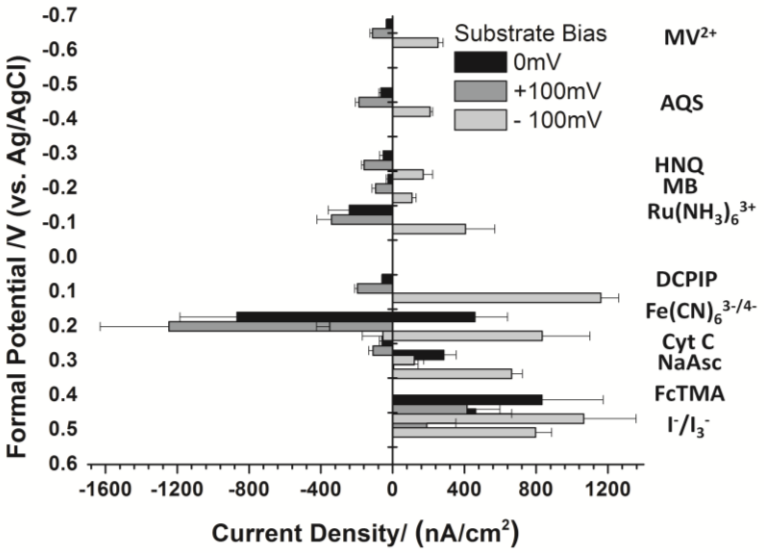

Figure 10. Photocurrent density of redox mediators at 0, 100, and -100mV overpotential coresponding to their formal potential (n=3). The concentration of each mediator is 200 μM, prepared in PBS solution with 100mM KCl.

Mixed Mediator Systems

In nature, two distinct electron transporters are used to shuttle electrons to and from the active sites of PSI, plastocyanin, and ferredoxin respectively. Thus, in order to simulate this dual ET process, mediators were mixed to investigate the possibility of increasing the efficiency of ET in a similar manner. There are four groups of mediators that were mixed in equal molar fashion for specific reasons. (1), MV / $Fe(CN)_6^{4-}$ is of particular interest because the $E^{0'}$ of MV is close to ferredoxin, while the $E^{0'}$ of $Fe(CN)_6^{4-}$ is close to plastocyanin (see Table 1); (2), $Fe(CN)_6^{3-}$/ $Fe(CN)_6^{4-}$, were chosen because $Fe(CN)_6^{3-/4-}$ is a well-known redox couple, and provides excellent

photocurrent for the PSI-based system individually; (3), DCPIP / NaAsc were selected because they were used frequently in PSI electrochemical studies; [17, 47, 48, 55, 56] (4), MV / Cyt C were used because Cyt C is a natural biological electron carrier, and MV has been coupled with Cyt C for an electrocatalysis study of PSI in solution and demonstrated to have a catalytic effect. [12] Assuming that the mediators do not interact with one another, the mixing of different mediators should broaden the active potential range of the system.[57]

Among these combinations of mediators, only MV / $Fe(CN)_6^{4-}$ generated a higher photocurrent density than their individual mediators at 0 mV overpotential. DCPIP / NaAsc showed enhancement in photocurrent at -100 mV overpotential, similar to DCPIP alone. Because NaAsc is a sacrificial electron donor, using it at the same concentration as DCPIP may prevent the system from performing in a cyclic fashion. In fact, most studies that use NaAsc in conjunction with DCPIP have examined at least 20 times more NaAsc than DCPIP.[8, 17, 48, 58] When this ratio was studied the photocurrents observed were higher than the individual components, but not 20 times greater than the lower ratio (data not shown). It is also worth noting that the addition of NaAsc to DCPIP significantly reduced the absorption of the mediator solution (Figure **11**). The photocurrent enhancement found through the use of combining MV/$Fe(CN)_6^{4-}$ provides evidence for the indirect electron transfer (IET) process, and suggests that using redox mediators in a biomimetic approach is a viable option for these systems. In addition, when oxygen is bubbled into the MV and MV/$Fe(CN)_6^{4-}$ solution, the photocurrent density is improved (data not shown), which agrees with the claim that PSI based photocurrent can be enhanced by oxygen, which can facilitate methyl viologen's ET by oxidizing MV^+ back to MV^{2+}.[50]

Table 2. The comparison of the photocurrent density between mixed mediator systems and their individual components

Mix Redox mediators	**J/(nA/cm^2) [c] of mixed mediators**			**J/(nA/cm^2) of e$^-$ acceptor**			**J/(nA/cm^2) of e$^-$ donor**		
Overpotential bias / mV	**+100**	**0**	**-100**	**+100**	**0**	**-100**	**+100**	**0**	**-100**
MV / $Fe(CN)_6^{4-}$	-285	613	1085	-111	-32	253	-350	458	834
$Fe(CN)_6^{3-}$/ $Fe(CN)_6^{4-}$	-792	-435	364	-1247	-867	-53	-350	458	834
DCPIP / NaAsc[a]	-229	71	1294	-159	-57	1169	-128	286	663
MV / Cyt C[b]	-125	-8	248	-111	-32	253	-109	-60	121

[a] DCPIP is an electron donor for PSI in this system, because it was reduced by NaAsc; and NaAsc is a reducing agent for DCPIP

[b] Cyt C is not an electron donor but an electron acceptor

[c] J is the average photocurrent density. Values represent the average of 3 samples

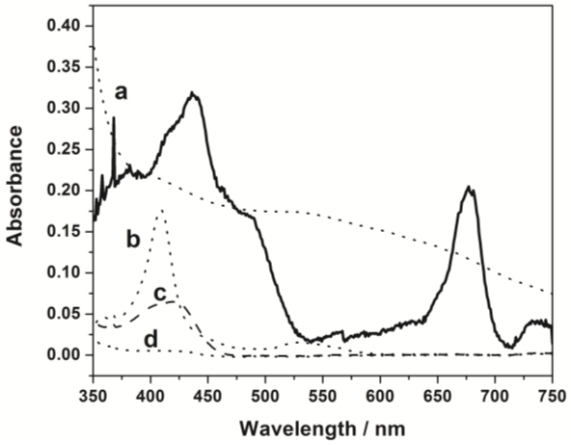

Figure 11. UV-Vis Spectra of mixed redox mediators (dotted line) and PSI solution(continuous line). The mixed solution contains 100 μM of each redox mediators. (a)DCPIP/NaAsc, (b) MV/Cyt C, (c) $Fe(CN)_6^{3-/4-}$, (d) MV/ $Fe(CN)_6^{4-}$ The PSI solution was prepared by diluting the dilalized solution by 50,the PSI absorbance data has been multiplied by 20, and (a) and (b) solution has been dilluted 50 times.

Mediator Concentration

Different concentrations of $Ru(NH_3)_6^{3+}$ were tested on PSI-modified electrodes to evaluate the relationship between mediator concentration and photocurrent density. $Ru(NH_3)_6^{3+}$ was chosen for this concentration study because it is very soluble in water, colorless, its $E^{0'}$ is nearly halfway between the formal potentials of P700 and F_B, and the photocurrent density of $Ru(NH_3)_6^{3+}$ in the

previous experiments was reasonable. Figure **12** demonstrates a linear relationship between photocurrent density and mediator concentration in the range of 2 to 90 mM (equation 1), as predicted by the Cottrell equation.[59]

$$Current\ Density\left(nA/cm^2\right) = \left(20 \pm 2\right) Ruhex\ Concentration + \left(274 \pm 35\right) \quad (10)$$

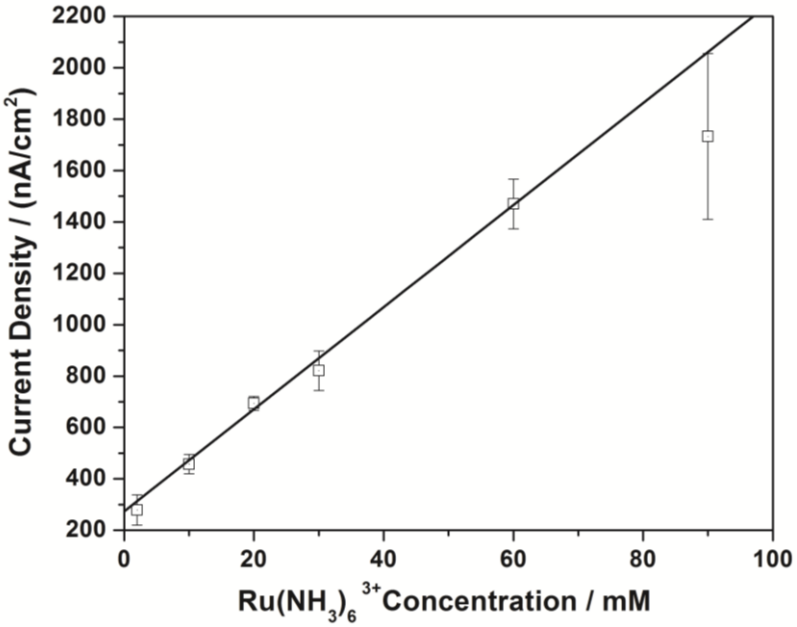

Figure 12. Photocurrent density for PSI modified gold electrodes as a function of various $Ru(NH_3)_6^{3+}$ concentrations (n=3). The solid line represents the linear fit of the data.

While the other studies in this paper were used at a concentration of 200 μM, this study demonstrates that the photocurrent density can be increased by increasing the concentration. In addition, the concentration vs. photocurrent density curve did not plateau until high concentrations were reached, implying that high mediator concentrations can be applied to obtain higher photocurrent densities when mediator cost is not a concern.

CONCLUSIONS

For the first time a series of redox mediators for PSI based system have been investigated that includes inorganic complexes, organic compounds, and biological materials with formal potentials that span the potential difference of P700 and F_B. The results demonstrate that the formal potential

and oxidation state of the mediator are key factors for photocurrent production. The results also suggest that the mediators' absorbance and concentration have a significant impact on the observed photocurrent density for this biohybrid system. The mediator that produced the largest photocurrent at equilibrium potential for the PSI based electrode investigated in this study was ferricyanide. Additionally, the use of a combined mediator system (MV/ferrocyanide) demonstrated the feasibility of a biomimetic approach for this system, and provided evidence for the proposed IET process. This study provides invaluable insights into the properties that researchers should consider while choosing an appropriate mediator for various electrochemical systems. Furthermore, this compilation of ET carriers implicates a useful approach for other bio-circuit systems.

ACKNOWLEDGEMENTS

We gratefully acknowledge the support of this research by the National Science Foundation (DMR 0907619), the NSF EPSCoR (EPS 10040083), and the Scialog Program from The Research Corporation for Science Advancement.

CHAPTER IV

REAL-TIME DETECTION OF MULTILAYER PHOTOSYSTEM I PHOTOELECTROCHEMICAL PROPERTIES BY SCANNING ELECTROCHEMICAL MICROSCOPY

As a result of the increasing global demand for clean and renewable energy, the integration of Photosystem I (PSI) proteins with electrode materials has become an intense area of research due to PSI's ability to convert solar energy into electrical energy with quantum efficiency near unity. PSI is a superabundant protein complex present in most oxygenic photosynthesis organisms that has been optimized through natural selection.[2] PSI, as a natural photodiode, performs two distinct redox processes at opposite ends of the protein complex. In nature, antenna pigments absorb incident photons, after which their energy is transported to the P700 reaction center. P700, a chlorophyll dimer, uses the light to energize electrons, which are then transferred to a terminal ion sulfur cluster denoted as F_B, resulting in charge separation. These electrons are used in nature to reduce ferredoxin, which provides electrons to a variety of crucial redox reactions in plants. At the other end, plastocyanin, a copper-containing protein, supplies electrons to reduce the excited $P700^+$.[2, 4]

The unique function and the potential for bio-mimetic devices of solar energy conversion make PSI an attractive nanoscale biomaterial for research. Research concerning immobilized PSI has progressed through the use of various methods including platinization of the terminal F_B acceptor[5] and self-assembly into thin films[6]. Other than these monolayer immobilization methods, our group has developed a rapid deposition method by applying a vacuum above the aqueous PSI solution to precipitate thick multilayer films of PSI which are able to enhance photocurrent.[17, 19] The mechanism of electrocatalytic investigation of light-induced electron transfer (ET) has been studied

in solution in the presence of cytochrome c6 and methyl viologen (MV).[12] Moreover, ET behavior of monolayer PSI films has been detected electrochemically.[13, 16] Furthermore, the enhancement of multilayer films of PSI has been studied using traditional three electrode electrochemical techniques.[19] However, due to the limitation of available instruments, previous electrochemical investigations regarding the nature of the ET process in these thick films and the communication among PSI reaction centers, mediators and electrodes were not discovered.

Scanning electrochemical microscopy (SECM) is a powerful tool in the study of heterogeneous ET reactions in biological systems.[34] In SECM experiments, a tip electrode (typically smaller than 25 μm in diameter) is moved across or approached toward the surface of a substrate electrode. The current depends on both distance from the substrate surface and the chemical and electrical properties of surface. In another words, SECM is a "chemical microscope" which provides electrochemical perturbations upon tip movement.[60] Several groups have utilized SECM to study plant photosynthesis or respiration processes, focusing on the oxygen profile during these processes.[61-64] Our group has applied SECM to image PSI that was absorbed on a micro-patterned gold substrate. Results indicate that PSI can be selectively adsorbed onto hydroxyl-terminated alkanethiolate self-assembled monolayer (SAM) rather than methyl-terminated SAM.[15] However, a complete SECM study concerning the redox properties of PSI, especially multilayer PSI films, has not been performed.

In this chapter, SECM has been employed to detect the photoexcited ET in multilayer films of PSI on a gold substrate electrode. The proposed scheme of the illumination experiments is shown in Figure **13**. During irradiation, the gold substrate electrode can either donate electrons to reduce the photooxidized $P700^+$ or the electrode can receive electrons from reduced F_B^- cofactors located near

the electrode surface. At the PSI/solution interface, mediators are required to maintain a steady flow of current by accepting electrons from F_B^- or donating electrons to $P700^+$ that are located near this interface. The redox mediator then travels via diffusion to the tip electrode where the electroactive products generated from substrate are converted back into their initial oxidation state. Here the conductivity of PSI in dark and light conditions was compared to completely conductive and insulating substrates. In addition, the first photoresponse of PSI in redox mediator solutions obtained by SECM is reported. The experimental results show the importance of the choice of substrate and tip electrode potential. These results provide insights for the utilization of multilayer PSI in nano-electronic devices and provides as an example for studies with other redox enzyme films in the future.

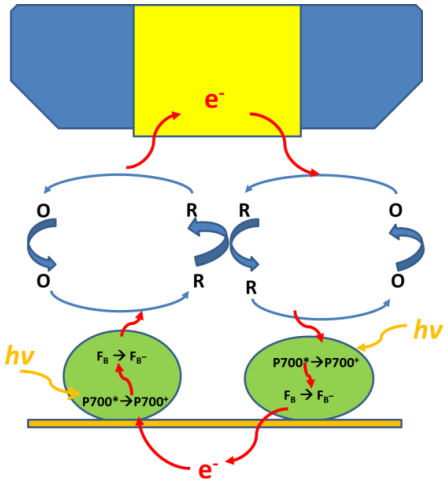

Figure 13. SECM scheme for PSI and redox mediator interaction. On the left, the gold substrate electrode donates electrons to reduce the photooxidized $P700^+$, while F_B^- offers electrons to reduce the oxidized species (O) and produce the reduced species (R); R is then oxidized at the tip electrode to regenerate O. On the right, the reverse process is depicted.

EXPERIMENTAL

Chemicals and Materials

The chemicals were purchased as follows: phosphate buffer, and H_2O_2 from Fisher Scientific; methyl viologen (MV), $K_4Fe(CN)_6$, 2-aminoethanethiol, and terephthalaldehyde (TPDA) from Sigma-Aldrich; H_2SO_4 from Merck; ethanol from PHARMCO-AAPER; N_2 from Gibbs Welding supply; gold wire from Goodfellow; conductive silver epoxy from Epoxy Technology; and white sealant Hysol Epoxi-Patch from Loctite. All chemicals are used as received unless otherwise specified. Solutions (1 mM) of 2-aminoethanethiol and TPDA were prepared in ethanol. The light source employed was a Dolan-Jenner Fiber Optic Illuminator Model 190.

PSI Extraction and Purification

PSI complexes were extracted from baby spinach as described previously.[16,19, 35-37] Briefly, thylakoid membranes were isolated via maceration followed by centrifugation using the method of Reeves *et al.*[36] coupled with several adaptations made by Ciobanu.[16] Second, PSI complexes were separated from the thylakoid membranes by additional centrifugation followed by purification using a chromatographic column packed with hydroxylapatite.[35, 37] Aliquots of 1 mL of the column effluent were then dialyzed in deionized water for 24 h using 10,000 MW cut-off dialysis tubing (Spectrapore), which reduced the initial concentrations of Triton X-100 (0.5 g L^{-1}), Na_2HPO_4 (0.2 M), and NaH_2PO_4 (0.2 M) to 0.25 mg L^{-1} , 0.1 mM, and 0.1 mM, respectively, assuming complete dialysis. The total chlorophyll concentration of the product was determined by the method of Porra *et al.*[38] to be 9.9×10^{-5} M with a Chl a/ Chl b ratio of 3.4. The P700 concentration was determined using the method of Baba *el al.*[37] to be 3.5×10^{-6} M, yielding a Chl / P700 ratio of 29.

Vacuum-Assisted PSI Multilayer Assembly

A 2 mm diameter gold disk electrode (CHI 101) was employed as the substrate electrode. The gold surface was cleaned with piranha solution (3:1 concentrated sulfuric acid: 30% hydrogen peroxide) prior to use, rinsed with distilled water and ethanol, and dried under a stream of nitrogen gas. The clean gold substrate was then immersed in 1 mM 2-aminoethanethiol solution for 1 h, rinsed with ethanol, dried by N_2 (g), and immersed in 1 mM TPDA for another hour, rinsed, and dried again. The TPDA-capped SAM functions to bind lysine residues on the two ends of proteins through covalent imine bonds.[35] The substrate was then placed in a vacuum chamber, and the liquid in the PSI was evaporated with the vacuum assistance. Additional layers of PSI films were subsequently deposited on the previous films in a similar manner. Three layers were immobilized in the following experiments.

Scanning Electrochemical Microscopy

The SECM experiments were performed with a CHI900 (CH Instruments, Inc. Austin, TX). The tip ultramicroelectrodes (UMEs) were fabricated and polished according to Bard *et al.*[34] The 2 mm Au disk electrode was polished with 0.05 μm alumina before modification with SAMs. Both the UME and the substrate electrode were acid cleaned in a 0.5 M H_2SO_4 solution prior to each experiment. The reference electrode was an aqueous Ag/AgCl (3 M KCl) from CH Instruments, Inc. The counter electrode was platinum wire (Goodfellow).

RESULTS AND DISCUSSIONS

In order to detect the ET kinetics in multilayer PSI, approach curves (AC) were performed under both dark and light conditions. As the tip approaches the substrate, either an increase (positive

feedback) or decrease (negative feedback) in the tip current will be observed, depending on whether the substrate exhibits conductive or insulative character, respectively. Other than these two distinct limiting cases, there is an intermediate situation where regeneration of redox species occurs at a limited rate.[65]

In our experiment, the variation of conductivity and electrochemical properties were measured at different spots. As displayed schematically in the Figure **14** B, half of the gold disk electrode was modified by multilayer PSI. This design assures that experiments with and without the PSI film are conducted under the same conditions, allowing for accurate comparison. The 50X optical microscope pictures are shown on Figure **14** C, indicating that assembly was not uniform, as a few remaining spots were not covered by PSI after three layers of deposition. All currents and distances were normalized for comparison purposes.

The experimental results demonstrated a negative feedback AC when the tip moved close to the insulating edge (Figure **14**A, curve IV), and a positive feedback AC when brought tip closer to the Au/SAMs (conductive) surface (Figure **14**A, curve I) as expected according to theory.[34] A current drop was observed as the tip moved closer to the substrate in the PSI region under dark conditions, showing a negative feedback. (Figure **14**A, curve III) This is consistent with our previous studies, demonstrated by Ciaobanu *et al.*[15] In the absence of optical illumination, the PSI films serve as an effective blocking layer causing the AC to demonstrate negative feedback as the tip approaches the substrate film.

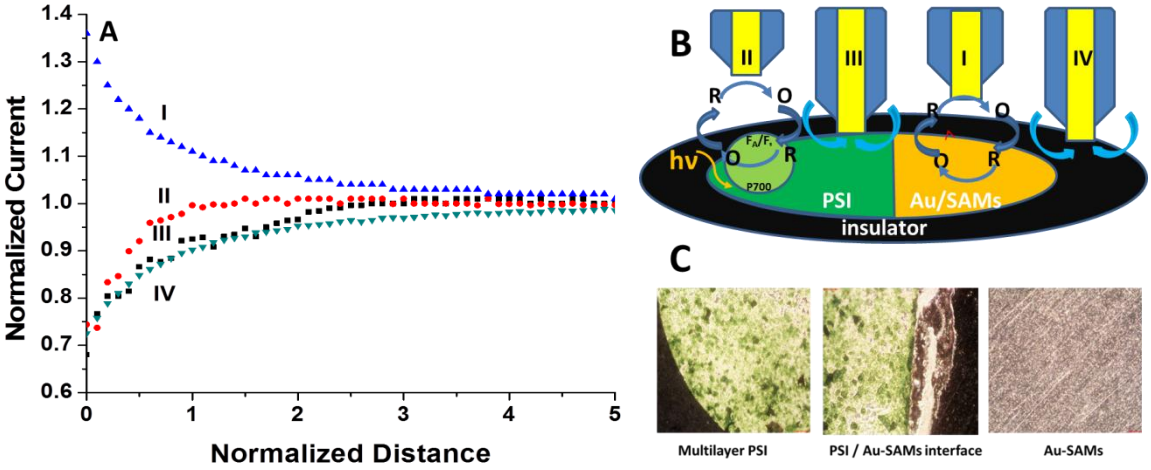

Figure 14. Approach curves at various spots (A) (Curve I, on top of Au; II on top of PSI under illumination; III on top of PSI under dark; IV on top of insulator edge); (B) Schematic diagram with the corresponding spots of the coated electrode and (C) Optical microscope pictures of multilayer PSI modified substrate. The microscope pictures were taken in dark field with 50 X magnification. Multilayer PSI was deposited by the vacuum-assisted technique; the other half of the electrode was covered by Teflon tape during deposition. The tip was immersed in 1mM $K_4Fe(CN)_6$ and 100mM KCl in PBS solution, and held at 0.45 V vs. Ag/AgCl; the substrate was unbiased. Approach speed was 0.5 μm μms^{-1}.

Under light conditions, however, the AC showed a steady (or slightly increased) current as the tip approached the PSI surface, indicating that the concentration of $Fe(CN)_6^{4-}$ was stable in the light induced PSI film while tip approaching. The sharp decrease of tip current at ~1 tip diameter in Figure **15**D, curve II is due to a blocking effect when the tip is about to touch the multilayer film. As shown in the scheme (Figure **13**), when light was turned on in the system, $Fe(CN)_6^{4-}$ was oxidized to $Fe(CN)_6^{3-}$ at the tip, and the excited F_B sites in the PSI film were able to offer electrons to the mediator solution to regenerate $Fe(CN)_6^{4-}$. However, the amount of the regeneration at the PSI surface has not equaled the consumption by the tip, so the positive feedback presented here is not obvious.[65, 66] The AC curves show that PSI multilayer film under illumination has neither completely conductive nor insulative character, but demonstrates a limiting regeneration rate of the mediator.

Photochronoamperometry was used to determine the photoactivity and provide insight into the photocurrent direction of the PSI film. In photochronoamperometry, the tip is positioned in close proximity (~1 tip diameter) to the substrate and a constant potential is applied to both the tip and substrate electrodes while the resulting current is measured under dark and light conditions. In general, the tip response is a function of the tip-substrate separation distance, *d*, and the relevant reaction kinetics, as well as the applied electrode potentials.

The tip and substrate potentials, E_T and E_S, respectively, determine the reactions that will take place at the electrode/solution interface. Prior to the experiment the tip is lowered to the surface by monitoring the current of the approach in which the predominant redox species, MV^{2+}, is reduced by the tip. When the tip was positioned near the substrate, it was set to a suitable overpotential for the collection of electrons from reduced mediator species (MV^{+}) generated by oxidation of the F_B sites. At the same time, the E_S was fixed at a value to promote reduction of P700 while remaining close to the cell open-circuit potential, in order to minimize background signal (Figure **15**A, B). Alternatively, the E_T can be biased towards more negative values, generating MV^{+} to reduce photo-excited $P700^{+}$, while the E_S is set to a value positive enough to gather electrons from F_B (Figure **15**C, D). The time at which the light was switched on and off is indicated by arrows. As can be seen from Figure **15**, photocurrent confirmed the functional photoactivity of PSI.

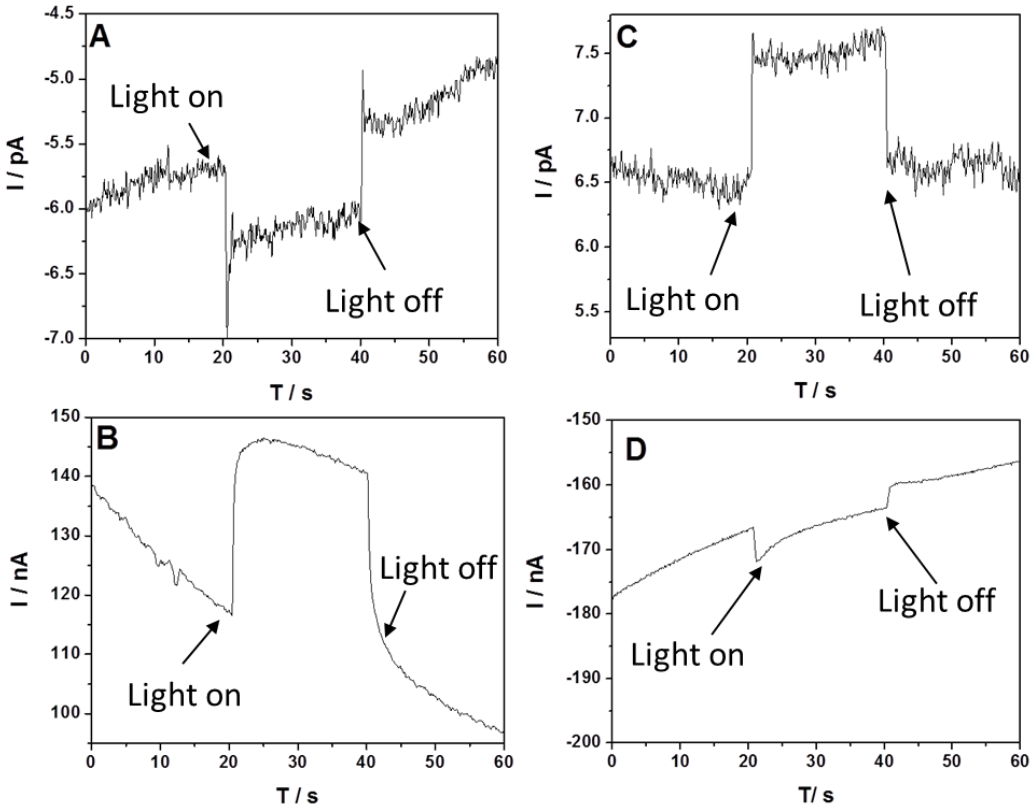

Figure 15. Photochronoamperometry for PSI in methyl viologen solution: A and C show the tip current while B and D show the substrate current. The light source was turned on from 20 to 40 s. A and B present the substrate generation/tip collection under the potentials E_T=0.2 V, E_s=0.1 V vs. Ag/AgCl (3 M KCl). C and D represent the tip generation/substrate collection; E_T=-0.1 V, E_s=0.3 V vs. Ag/AgCl (3 M KCl). The mediator used was 200 μM MV^{2+} and 100mM KCl in PBS solution.

As described in Figure **13**, for individual photoactive PSI, if the P700 reaction center is located near the substrate electrode during irradiation, the gold substrate electrode can donate electrons to reduce the photooxidized $P700^+$, and the electrons that transfer to the F_B site can reduce the MV^{2+}, resulting in increased cathodic substrate current. Increased anodic current is observed at the tip, corresponding with electrons flowing into the tip electrode. If F_B site is located near the substrate electrode, the substrate electrode can receive electrons from the reduced F_B^- cofactor during irradiation, resulting in increased anodic current at the substrate. The reduced MV^+ in the mediator solution donates electrons to $P700^+$, regenerating P700. The tip reduces the generated oxidized

species in solution, resulting in increased cathodic current. In the present study, there are many possible orientations for the PSI proteins stacked in the multilayer film, as well as their interactions with the redox mediators. The fact that both anodic and cathodic photocurrents are observed implies that the orientation of the protein complex is mixed in the multilayer film, as expected. The results also suggest that ET in the multilayer film can act as an integrated device, and can be controlled by the applied electrode potential.

CONCLUSIONS

In summary, the electrochemical and photoelectrochemical behavior for a multilayer film of PSI has been determined by SECM. This is the first time that photo responsive current has been simultaneously observed for both redox processes of PSI using SECM. The results also indicate that with the current immobilization method, although PSI was in a mixed-orientation. Approach curves demonstrated that the ET of PSI in light conditions exhibited a limiting regeneration rate for the mediator. Future studies will utilize nano-scale ultramicroelectrode in order to detect individual PSI orientation.

ACKNOWLEDGEMENT

We gratefully acknowledge the financial support from the National Science Foundation (DMR 0907619) and the NSF EPSCoR (EPS 10040083), and the Scialog Program from the Research Corporation for Science Advancement.

CHAPTER V

INVESTIGATION OF THE CATALYTIC ACTIVITY FOR HYDROGEN PRODUCTION ON PLATINIZED MULTIALYER PHOTOSYSTEM I FILMS WITH SCANNING ELECTROCHEMICAL MICROSCOPY

The electrocatalysis of hydrogen production is a fascinating area in research, due to the energy conversion and clean energy produced in this reaction. Unfortunately, current methods for producing hydrogen are inefficient and often utilize carbon based energy sources. In addition, the $2H^+ + 2e^- \rightleftarrows H_2$ reaction is only kinetically favorable on certain noble metals such as Pt, Ru, or Rd.[67] Among these noble metals, platinum is one of the best catalysts for hydrogen oxidation and proton reduction. Platinum coupled with Photosystem I (PSI), a protein complex present in most photosynthetic organisms, has been used to directly convert solar energy into hydrogen energy.[68-72] In nature, the antenna pigments absorb the incident photons, and the photons will be transported from antenna chlorophylls to P700 reaction center. P700 is a chlorophyll dimmer that accepts photons and energizes electrons result in charge separation. The electrons generated here will travel through an electron transfer chain. The end of this chain is an iron-sulfur cluster denoted as F_B which reduces ferredoxin, and the reduced ferredoxin will provides electrons in a variety of redox reactions in plants. In these studies, the electrons from the F_B were utilized to first precipitate platinum and subsequently for hydrogen production.

Previously, the characterization methods of bio-hybrid catalysts for hydrogen generation either employ gas chromatography,[68, 70, 72] or tin oxide hydrogen sensor[69, 71]. However, these detection methods only offer bulk information about the hydrogen production. Here we employed the use of a Scanning Electrochemical Microscope (SECM) to probe on the substrate surface and image the

catalytic active sites directly. This provided us with a much more detail picture of the catalytic activity occurring at the protein/catalyst/solution interface.

We immobilized multilayer films of PSI to photoreduce platinum on the surface of the protein film following the reaction: $[PtCl_6]^{2-} + 4e^- \xrightarrow{h\nu} Pt_{(s)} + 6Cl^-$. The platinum was photoreduced on to the bio-hybrid electrode with and without the use of sodium ascorbate (NaAsc) as a sacrificial electron donor. NaAsc is able to reintroduce electrons to P700 after the reduction process, resulting in multiple electron turnover events from each PSI complex. The resulting bio-hybrid film was firstly characterized using scanning electron microscopy (SEM), and energy dispersive X-ray spectroscopy (EDX). SEM images demonstrate that particles are scattered on the substrate surface in various sizes, some up to several micrometers. The EDX result confirmed that these particles are platinum. Finally, SECM experiments were used to demonstrate the catalytic ability of these particles for the H^+/H_2 redox couple. In these SECM experiments, a tip was scanned across the platinized PSI surface both under substrate generation / tip collection (SG/TC) mode and tip generation / substrate collection (TG/SC) mode. Under SG/TC mode, the protons were reduced to hydrogen on the platinized PSI substrate, and then oxidized back to protons at the tip. The SECM image showed increased cathodic current when light was turned on for the substrate, while an increase of anodic current was observed for the tip. The TG/SC mode has performed a reverse process. By utilizing a smaller UME, we were able to image individual platinum particles present on the surface of the multilayer film. These results demonstrate how SECM can be utilized to image the redox chemistry of a functional bio-hybrid device.

EXPERIMENTAL

The platinized PSI multilayer substrate electrodes were prepared by Gabriel LeBlanc in our group, and more detailed characterization can be found from the Langmuir paper.[73] Briefly, the extracted PSI solution was placed on the substrate and vacuumed to dryness. This vacuum deposition process was repeated 3 times in order to generate thick multilayer films of PSI.[19] To photoreduce platinum onto the protein, the dried substrate was immersed in a platinate salt solution. Upon illumination, electrons are excited from the P700 reaction centers and travel down the electron transfer chain to the F_B site, and then used to reduce the platinum from its original oxidation state (II or IV) to zero.

SEM and EDX analyses were performed on a Hitachi S-4200 instrument. SEM images were collected with an accelerating voltage of 20 kV. EDX analyses were performed using an accelerating voltage of 20 kV and an emission current of 20 μA.

SECM experiments were performed on a CH Instruments CHI 900 electrochemical workstation. Platinum ultramicroelectrode (UME) was used as the tip electrode and a platinized PSI-gold sample (2 hrs photoreduction time) described previously as the substrate electrode. A 100 mM KCl solution adjusted to a pH of 4 using HCl was used as the mediator solution. The tip and substrate potential were set at their respective open circuit potential values. A step size of 10 μm was used with the tip brought near the substrate electrode using a feedback approach curve technique.

RESULTS AND DISCUSSION

Confirmation of photoreduced platinum by SEM / EDX

SEM / EDX has been used to confirm the existing of photoreduced platinum in both with and without NaAsc sacrificial electron donor environment. As seen in Figure **16** A, platinum particles

are scattered over the surface of the sample. Performing EDX directly on one of these particles (as indicated by the arrow) revealed a strong platinum signal (Figure **16** C). The presence of various sized platinum regions would indicate that photoreduction begins with a small nucleation event, presumably at the F_B site, which then allows for larger platinum regions to form as electrons are continually fed to the platinum particles by the protein complexes. This is supported by previous reports of smaller platinum particles when photoreduction occurs in the PSI solution.[68] Furthermore, when EDX analysis was performed on the darker regions of the SEM image, the platinum signal was greatly reduced in comparison to the bright areas, suggesting the presence of smaller platinum particles. The ability for particle growth appears specific to this immobilized PSI photoreduction technique.

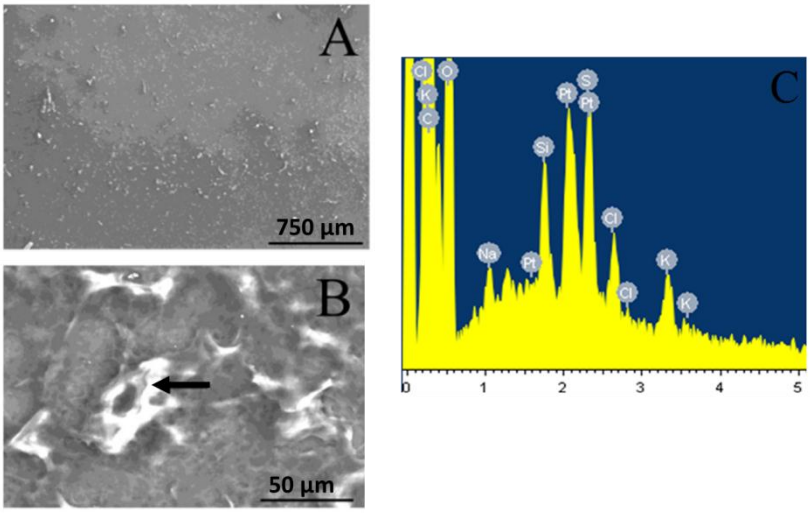

Figure 16. SEM and EDX image of platinized PSI with using NaAsc**.** A: SEM image demonstrates a large number of platinum particles present on the multilayer PSI surface. B: magnified SEM picture of A. C: EDX analysis performed directly on the point indicated by the arrow in B. The EDX used an accelerating voltage of 20 kV and emission current of 20 µA.

Interestingly, multilayer films of PSI are capable of photoreducing platinate salts to platinum particles without a sacrificial electron donor. Figure **17** A, B shows the dispersion of platinum

particle on the platinized PSI sample, as well as the variation of platinum particle sizes from nanometer to micrometer. The EDX was performed directly on particle indicated with arrow as (1), and confirmed the existence of platinum (Figure **17** C). The area around the particle showed no Pt (Figure **17** D). Though less platinum (0) is produced due to the limited number of electrons present in the film, this data suggest that electrons from proteins within the thick PSI film can be transferred to surrounding PSI molecules.

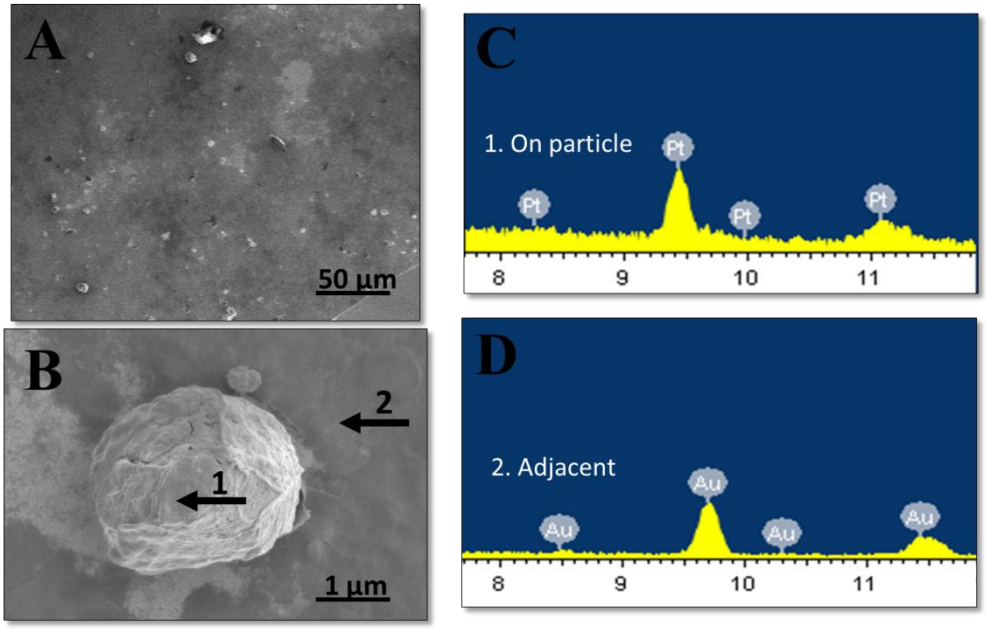

Figure 17. SEM and EDX image for platinized PSI without using NaAsc. A: SEM image demonstrate large number of platinum particles present on the multilayer PSI surface. B: magnified SEM picture of A. EDX analysis performed directly on particle (C) and adjacent area (D) as indicated by arrows. The EDX used an accelerating voltage of 20 kV and emission current of 20 µA.

Determination of platinum particle catalytic ability for hydrogen production by SECM

The purpose in this experiment was to use SECM coupled with the specific $2H^+ + 2e \overset{Pt}{\leftrightarrow} H_2$ reaction to distinguish spots with or without platinum on the platinized PSI substrate. SECM is able to probe a variety of electrochemical reactions and characterize the topography and redox activities

of the electrode-electrolyte interface. Here, we used SECM to characterize the properties of Pt electrocatalysis, and imaging platinized PSI with SG/TC and TG/SC mode.

First, cyclic voltammetry was employed to characterize the tip and to find a suitable pH. Tests were taken on a 2 mm diameter Pt disk electrode and 10 µm Pt UME. As shown in Figure **18** A, the pH 1.3 HCl solution with 100 mM KCl as supporting electrolyte displayed a typical voltammogram in 'S' shape for UME. This voltammogram showed a steady-state current in the range of potentials between 0.2V and -1.2 V vs. Ag/AgCl (3 M KCl), which indicates a diffusion-controlled current resulting from the proton reduction process ($2H^+ + 2e^- \rightleftarrows H_2$) in bulk solution. However, to avoid damaging the PSI films in the highly acidic solution, a mediator pH of 4 was applied in the image collection experiments.

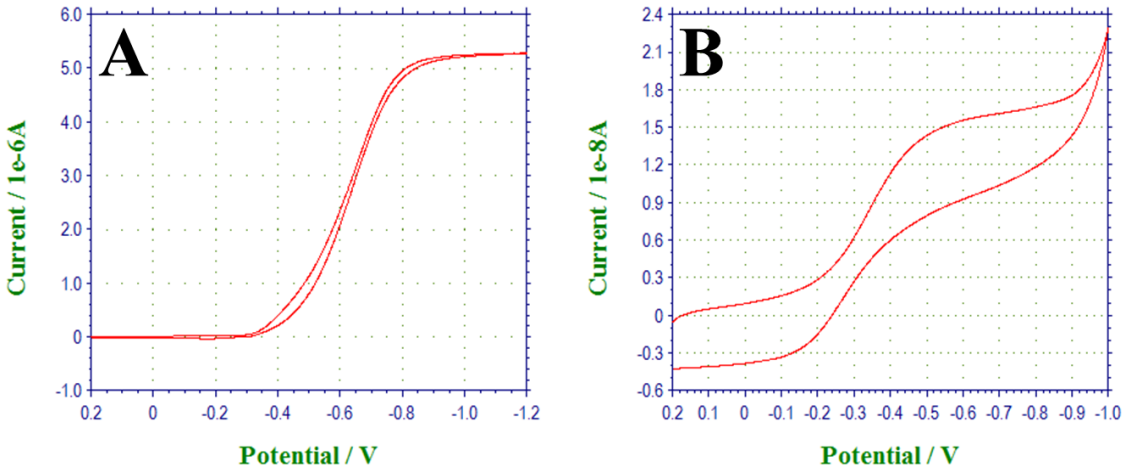

Figure 18. Cyclic Voltammograms recorded on 2 mm platinum disk electrode with 10 **µm** Pt UME. A: steady-state voltammogram was obtained in pH 1.3 HCl and 100mM KCl solution. B: voltammogram in pH 4.5 HCl and 100 mM KCl solution. Scan rate was 0.05 V s^{-1}.

Second, H^+/H_2 redox mediator feedback behavior on different substrates were analyzed with approach curve. As shown in Figure **18**, the proton reduction diffusion limit current was obtained when the potential is more negative than -0.8 V, and hydrogen oxidation steady-state current was

achieved in the potential range above -0.2 V in the voltammogram. Therefore, in the approach curve experiments, the tip was held at -0.8 V vs. Ag/AgCl, and substrate was held at -0.2 V. In contrast to traditional mediator systems, such as $Fe(CN)_6^{3-/4-}$, the H^+/H_2 couple displays a negative feedback on most conductive substrates, except for catalytic metals such as platinum.[74] A positive feedback approach curve appeared when the tip was moved close to a platinum disk electrode as expected, demonstrating fast oxidation of hydrogen and regeneration of proton on the substrate. On the other hand, the platinized PSI substrate without using NaAsc exhibited a negative feedback (Figure **19**) which indicated that the substrate was a non-catalytic surface for hydrogen oxidization. In other words, this suggests that no regeneration of tip-generated species occurred on most of the substrate area. This phenomenon is in good agreement with the SEM of platinized PSI (Figure **17** A) where a majority of the surface is not covered by platinum particles.

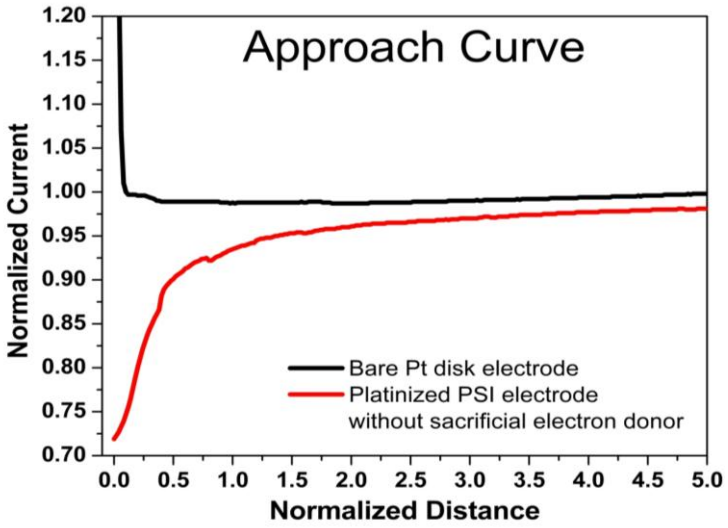

Figure 19. Approach Curve on bare platinum disk electrode (black line) and on platinized PSI without using NaAsc (red line). The tip was immersed in pH 1.3 HCl with 100 mM KCl solution, and held at -0.8V, and substrate was held at -0.2 V vs. Ag/AgCl. Approach speed was 0.05 μm s^{-1}.

Finally, catalytic activity of platinized PSI has been imaged by SECM in both SG/TC and TG/SC modes. The tip was a Pt UME; the substrate was the platinized PSI on a modified planar gold electrode, and the mediator solution was a 100 mM KCl solution brought to a pH of 4 using HCl. SECM (SG/TC) experiments were performed to demonstrate the catalytic ability of the photoreduced platinum present on the biohybrid electrode. Under these conditions, the protons in solution are converted to hydrogen by the catalytic platinum particles on the substrate surface and then converted back to protons via the tip. When the light is turned on (the region between the arrows), electrons are excited and transferred to reduce H^+, the substrate current becomes more cathodic while the tip current becomes more anodic. Once the light is turned off, the current for both the tip and the substrate returned to their original values (Figure **20**). The image indicates that the hydrogen production of these catalytic platinum particles occurs during light exposure. However, to avoid tip crash on the Pt particles, the tip was withdrawn 50 µm, which is too far away from the substrate to observe individual Pt particles.

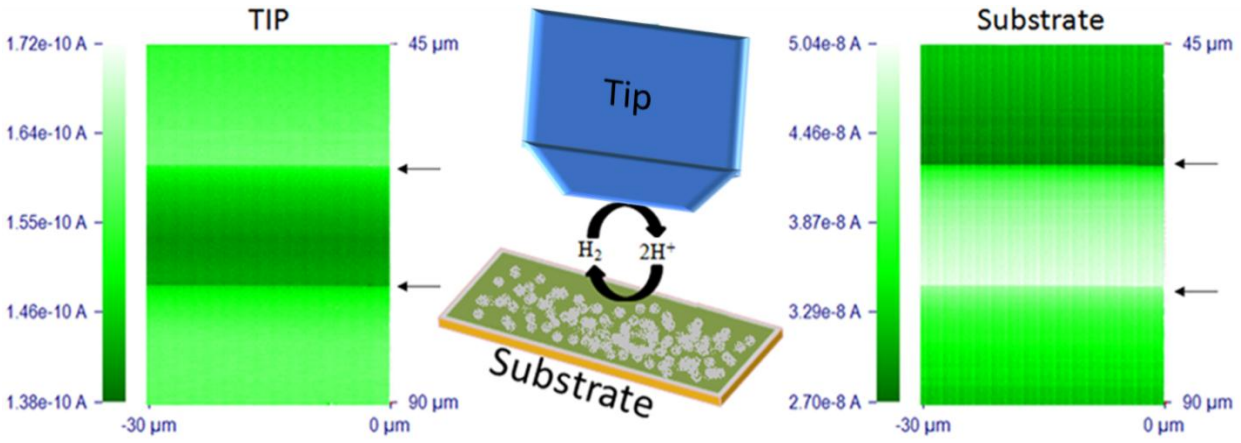

Figure 20. SECM SG/TC images of platinized PSI. A 25 µm platinum UME was on top of a three layer PSI that was platinized. The solution was pH 4 HCl and 100 mM KCl in DI water. The image was taken at E_T=-0.2 V, E_S=0.23 V. vs. Ag/AgCl (3 M KCl). Light was turned on as indicated by the arrows.

A (TG/SC) image was collected with a smaller tip (10 μm) closer to the substrate surface in order to electrochemically image individual platinum particles. At this distance a feedback current is produced as the tip passes above the catalytic particle, producing a significant increase in current. The red peaks in Figure **21** indicate "hot-spots" of electrochemical activity, indicating the location of photoreduced platinum particles. The sizes of the red peaks were several micrometers. As we can see from the SECM image, there are large areas of increased current present on the surface of the protein film that correspond well with the size of platinum particles observed in the SEM images (Figure **16**). "Tails" can be observed following each of these platinum particles due to scan direction of the tip. These "tails" are caused by the diffusion of electrochemical products away from the catalytic particles, enabling the feedback loop to continue beyond the physical dimensions of the particles themselves.

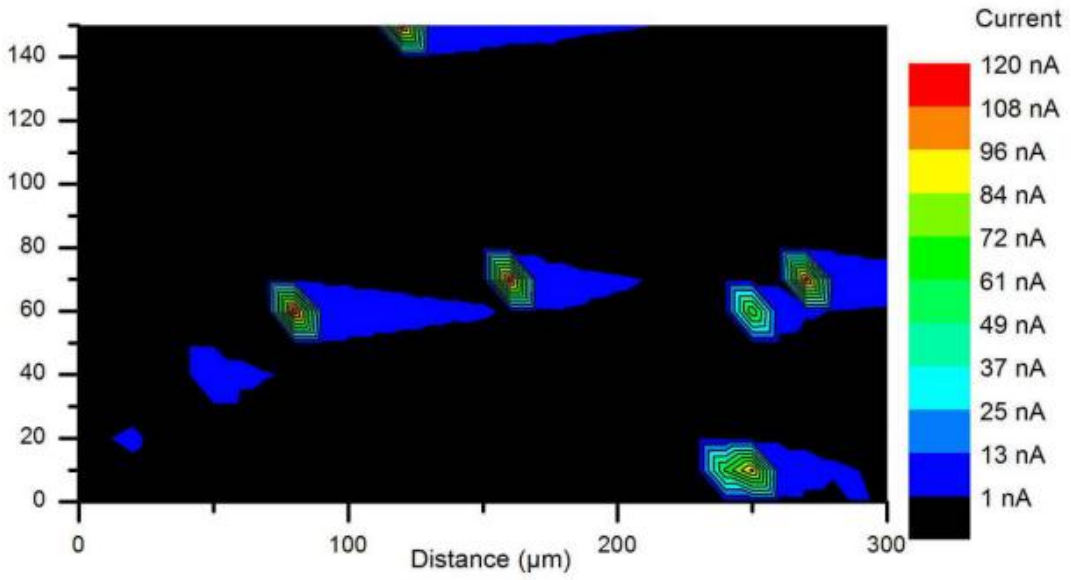

Figure 21.SECM TG/SC images of platinized PSI. A 10 μm platinum UME was on top of a three layer PSI that was platinized. The solution was pH 4 HCl and 100 mM KCl in DI water. The image was taken at E_T=-0.28 V, E_S=0.4 V vs. Ag/AgCl (3 M KCl). Hot spots (red to green color) showed platinum particle positions.

We were also able to image the small platinum particles produced without a sacrificial electron donor using a similar method. These particles did not have “tails”, most likely due to the lower scan rate used to produce the image. The size of the hot spot areas, also correspond well with the size of platinum particles observed in the SEM image for the PSI samples platinized in the absence of NaAsc (Figure **17**). In addition, there were some areas which showed continuous high current (red bands, Figure **22**) due to the overlapping electrochemical activity of several platinum particles.

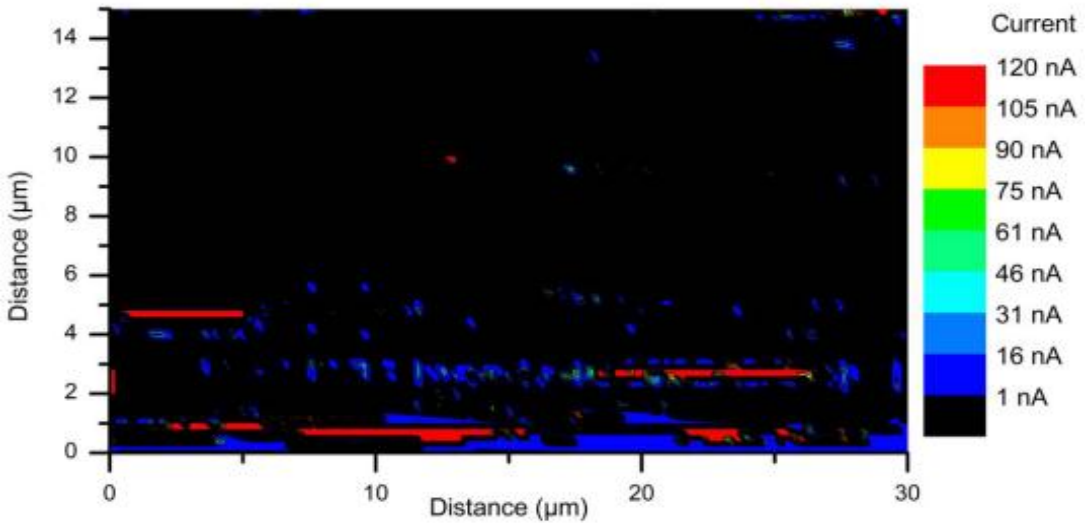

Figure 22. SECM TG/SC images of platinized PSI without NaAsc. A 2 µm platinum UME was on top of a three layer PSI that was platinized. The solution was pH 4 HCl and 100 mM KCl in DI water. Image was taken at E_T=-0.8 V, E_S=0 V vs. Ag/AgCl (3 M KCl). Hot spots (red to green color) showed platinum particle positions.

CONCLUSION

The SEM and EDX analysis of platinized PSI has demonstrated that PSI is capable of reducing platinum ions into platinum particles in a photocatalytic manner. The catalytic activity for hydrogen production of platinum particles has been interrogated by SECM. This study demonstrated the powerful of SECM to detect catalytic sites on a substrate surface, and also shows a promising future of building a higher efficiency fuel cell with platinum coupled PSI devices.

ACKNOWLEDGEMENT

We gratefully acknowledge the financial support from the National Science Foundation (DMR 0907619) and the NSF EPSCoR (EPS 1004083) from the Research Corporation Scialog Program for Science Advancement. Additionally we would like to acknowledge useful discussions with Dr. Peter N. Ciesielski and with Professor Barry D. Bruce of The University of Tennessee Knoxville.

CHAPTER VI

INVESTIGATION OF THE DISSIMILARITY METAL REDUCTION (DMR) PATHWAYS OF SHEWANELLA WITH SPATIAL RESOLUTION BY SCANNING ELECTROCHEMICAL MICROSCOPY

Shewanella oneidensis bacteria have recently gained attention due to their inherent ability to utilize insoluble metals as respiratory substrates. These substrates include organic compounds, and toxic metals.[25] Since insoluble substrates cannot freely diffuse into the cell, *Shewanella* must exhibit a capability of transferring electrons between these insoluble substrates and the cellular interior. *Shewanella* sp. are able to generate current on electrodes,[75] and oxidize electrodes to potentially drive a metabolic reaction.[76, 77] The biggest question researchers have is how electrons were transferred over a long distance from the cellular interior to a substrate that cannot freely diffuse to the cytoplasm. To move electrons over distances longer than 0.01 μm requires a specific pathway,[78-80] however previous studies shows that *Shewanella* is able to move electrons to metals located longer than 50 μm away from the cell surfaces. These experiments show that *Shewanealla* were able to reduce Fe(III) oxide which was precipitated in side of alginate beads or nano-porous glass beads regardless of the fact that the bacteria were too large to access the interior of the beads.[29, 30] In order to determine if direct contact between *Shewanella* and electrodes is required in the extracellular respiration, Jiang *et al.* performed an experiment showing that the current produced by *Shewanella* was similar, regardless of the cell contact. This experiment also suggested that the electron transfer (ET) involved a soluble electron shuttle.[32] Various mechanisms about how electrons are transferred over long distances have been proposed,[81, 82] however, more evidence supports the dissimilartory metal reduction pathway (DMR) pathway for electron flow, which

include direct and indirect pathways.[33] The direct pathway, which is composed of a series of multiheme cytochromes and transmembrane proteins (Metal reduction 'Mtr' pathway) facilitates electron movements from the cellular interior to the exterior.[83] The indirect pathway involves the secretion of soluble flavins, which have been shown to accelerate extracellular ET.[31, 32] The flavin has been identified by Marsili *et al.* by liquid chromatography– mass spectrometry (LC-MS). However, direct *in situ* detection of current through specific DMR pathways is a challenge for conventional analytical instruments.

Here, we use scanning electrochemical microscopy (SECM) to detect the direct and indirect DMR pathways. SECM is a powerful chemical microscope with high spatial resolution, allowing real time monitoring of ET about substrate chemical reactivity as well as topography. Moreover, SECM provides fine control over the potential, as well as distance between the tip and substrate electrode.[34] This is particularly useful when determining redox species in the cellular environment with small redox potential diversities. According to the previous results, the direct *Shewanella* DMR pathway is slower than the indirect pathway and occurs at higher potential.[84] SECM will directly collect current of specific DMR pathways for a real-time comparison of both pathways.

In addition, SECM substrate generation / tip collection mode will be used to monitor the cellular viability and flavin concentration when culturing bacteria under various growth conditions. *Shewanella* has been shown to form biofilms on different substrate electrode materials (graphite, Indium tin oxide, glassy carbon, iron minerals) when exposed to a bias around +0.2 V vs. NHE. Additionally, flavin has been demonstrated as an important soluble mediator and electron shuttle for *Shewanella*.[31] In this project, the combination of electrochemical technique and LC-MS studies of *Shewanella* biofilm supernatant has reconfirmed that the riboflavin is involved in the electron

shuttling process. The ability of quantitative detection of the SECM tip has been employed to detect the flavin secretion by *Shewanella* biofilm. The approach curves in vertical direction and horizontal line-scan studies in SECM have compared the redox activity of the biofilm in different mediators. Studies about direct ET pathways in *Shewanella* biofilms will be performed in the near future. The results will amplify our understanding and capability of distinguishing between the DMR pathways and the function of flavin in these pathways. This understanding will facilitate the optimization and utilization of *Shewannella sp.* for bioenergy, electrosynthesis and bioremediation applications.

EXPERIMENTAL

Materials

All chemicals were used as purchased without any further purification. Riboflavin, sodium lactate and fumarate were purchased from Sigma Aldrich. Pt wire was purchased from Goodfellow (Cambridge, UK). Ag/AgCl reference electrode was purchased from CH instrument. Ferrocenylmethyl-trimethylammonium hexaflorophosphate (FcTMA) was prepared according to the method of Mirkin and co-workers.[15, 52]

Microbiological Methods

S. oneidensis MR-1 were grown from -80 °C glycerol frozen stock by culture on lysogeny broth (LB) agar plate, and then inoculating 3 mL of LB broth (Sigma-Aldrich) with shaking (175 rpm) in air overnight at 30 °C. The culture was then centrifuged at 6000 rpm for 10 min to remove supernatant. The cells were washed and suspended in minimal media. The medium was prepared as in reported previously[31] and purged with N_2 for 30 min before being autoclaved. Afterward, casamino acids and 20 mM sodium lactate and 20 mM fumarate were added.

Analytical Methods

All the electrochemical measurements were performed with scanning electrochemical microscopy (SECM, CHI 900, CH Instruments). A 7 μm carbon fiber electrode was used as the SECM tip. Details about SECM tip fabrication could be found in literatures.[34] Pt wire and Ag/AgCl was used as counter and reference electrode respectively.

Electrochemical Measurements were carried out with CHI 900. A constant potential of 0.02V vs. Ag/AgCl (0.24V vs. NHE) was applied to the substrate electrode for 1 hour to form the biofilm.

After the biofilm has been formed on the substrate electrode, the medium is taken out and centrifuged. The supernatant is then injected into the electrochemical cell before the approach curve was taken over the biofilm in the medium solution, with holding the tip at -0.6 V, while biasing the substrate at -0.2 V vs. Ag/AgCl. To detect the concentration of riboflavin, square wave voltammetry (SWV) was employed, where the tip was fixed at 20 μm away from the biofilm, recording every 30 min. Background current using SWV was measured above the biofilm by an SECM tip.

For X-scan experiments, the biofilm was formed with a strip shaped mask on the glassy carbon electrode. The X-scan was followed by the approach curve experiments, and the tip was held 20 μm away from the substrate. The tip was than scanned at1.5 μm/s in the x-direction. Approach curves were performed using riboflavin or FcTMA as mediator.

For liquid chromatography – mass spectrometry (LC-MS), the cell-free culture supernatant of *Shewanella* biofilm solution was analyzed by electrospray ionization -triple quadrupole in the positive and negative scan mode at the range of 150-2000 mass to charge ratio.

RESULTS AND DISCUSSION

Biofilm formation

A biofilm community is a form in which natural bacterial populations present in high-density, low-cell number. In this form, bacteria are attached to a surface or to each other, and surrounded with extracellular aggregated matrix. Biofilms are spatially heterogeneous in chemical gradients and bacterial phenotypes. This heterogeneity has important implications on biological results due to the ability of diverse community to challenge external stresses.[85-87]

Shewanella species are able to form biofilm on a various electrodes, using electrodes as electron acceptors for respiration.[75] Figure **23** shows the formation of a *Shewanella* biofilm on a glassy carbon substrate electrode. It was biased at + 0.24 V vs. NHE, a stable oxidation current of about 10 nA has been observed in 60 min.

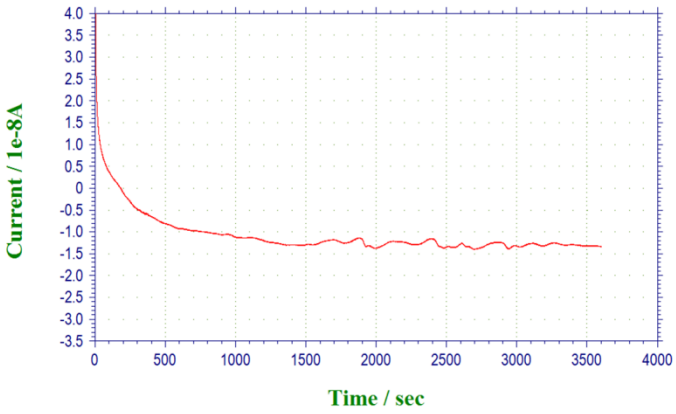

Figure 23. Chronoamperometry shows *Shewanella* biofilm formation in 60 min. The glassy carbon electrode was poised at + 0.24 V vs. NHE.

Identification of soluble mediator by SWV and LC-MS data showing evidence for riboflavin at the biofilm-electrode interface

Previous studies showed that when the medium was removed after biofilm formation and replaced with fresh medium, the current decreases sharply. However, after refilled with the

centrifuged medium supernatant, the current returned close to the original one.[31] This suggested that the dramatic increase in current with the replacement of cell-free culture supernatants demonstrated that the majority of measured current dependent on the presence of the soluble mediator. Our square wave voltammetry (SWV) experiment shows that the peak current in the 60 min biofilm solution decreased dramatically after replaced with fresh medium. The shape of the SWV is very similar with that of a 50 μM riboflavin solution. The shifted potential in the biofilm solution might be caused by the mix of oxygen or other mediators contained in the solution (Figure **24**). This result is consistent with the study performed by Marsili *et at.*, which showed the existence of soluble redox mediator secreted by the *Shewanella* biofilm, potentially riboflavin.[31]

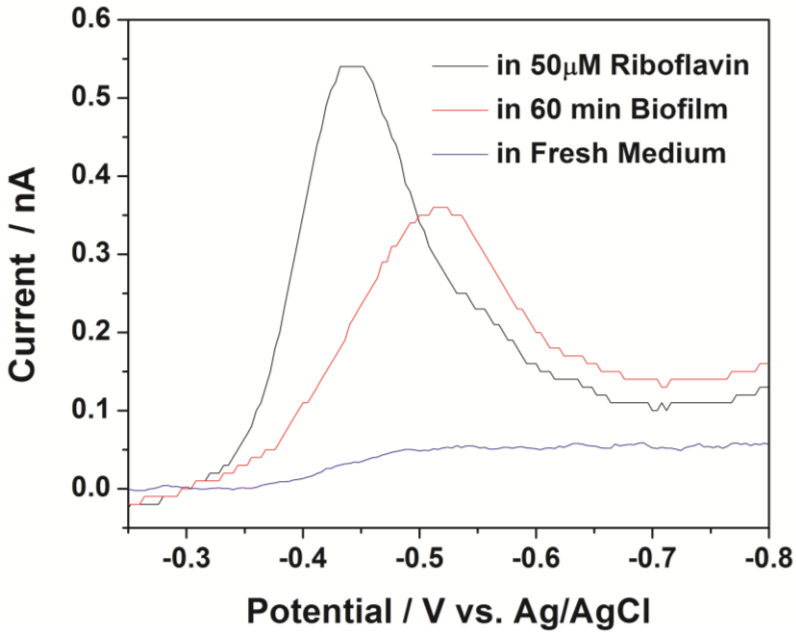

Figure 24. SWV of riboflavin produced by *Shewanella* biofilm and in 50 μM riboflavin. SWV was recorded by 7 μm carbon fiber tip in real-time at 20 μm distance from the biofilm surface. Counter and reference electrode was Pt wire and Ag/AgCl, respectively.

The identification of this soluble mediator was performed with LC-MS. The supernatant from 60 min biofilm, was studied using LC-MS, where a mass-to-charge ratio (m/z) of 376, identical to protonated riboflavin, was detected (Figure 25). Riboflavin, which has a molar mass of 377, is a

soluble redox mediator and also weakly chelate metals.[88] A chelator could bind to metal oxides, which will facilitate extracellular respiration.

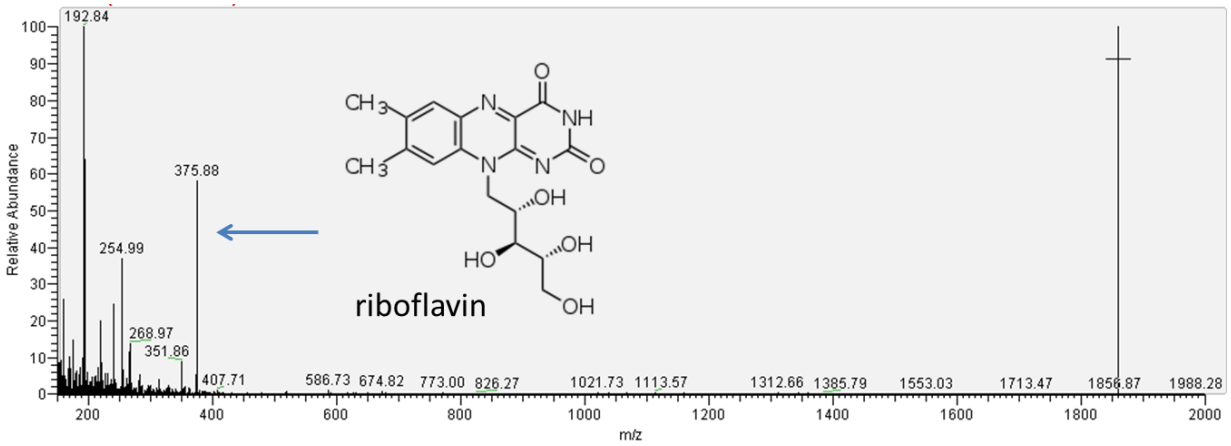

Figure 25. LC-MS results of riboflavin produced from *Shewanella* biofilm after 60 min formation.

Real-Time quantitative detection of riboflavin

The detection of a riboflavin concentration gradient within the biofilm will advance the understanding of extracellular ET in *Shewanella*. The primary challenge is the ability to quantify and spatially resolve the concentration profile of this small molecule immediately surrounding biofilms in real-time. The tip can be set at a static distance from a biological substrate, and measure the local concentration of redox active molecules over a biofilm. Riboflavin was the target redox active molecule in this study due to its involvement in extracellular electron shuttle as discussed in the previous section.

The riboflavin concentration calibration curve was obtained by detecting 5, 10, 20, 50, and 100 μM riboflavin prepared in *Shewanella* media (Figure **26**A). SWV was recorded at each riboflavin concentration with a 7 μm carbon fiber tip located in bulk solution. The parameters for SWV were as follows: initial potential: -0.2 V, final potential: -0.8 V, increment potential: 0.004 V, amplitude: 0.025 V, frequency 15 Hz.

Figure **26** B shows the formation of riboflavin by *Shewanella* biofilm as a function of time over the course of 30 min. The time point of 0 min represents the replacement of fresh medium with the old supernatant solution after the initial 60 min biofilm formation. Each concentration point in the plot corresponds to the SWV peak current. The concentration was calculated from the current recorded with riboflavin calibration curve with the linear fit equation (1).

$$Current = (1.63 \pm 0.34) \times 10^{-10} \times [riboflavin] + (5.77 \pm 0.67) \times 10^{-12} \quad (11)$$

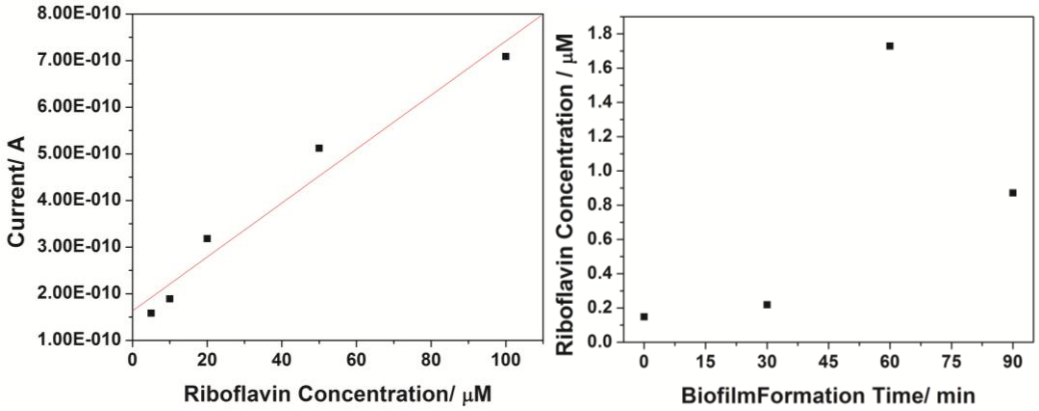

Figure 26. (A) Calibration curve at various concentrations of riboflavin (5-100 μM) in *Shewanella* medium. (B) Plot of real-time quantitative detection of riboflavin concentration produced by *Shewanella* biofilm as a function of time. Working electrode: 7 μm carbon fiber tip; Counter: Pt wire; Reference: Ag/AgCl.

As Figure **26** B shows, the concentration of riboflavin secreted by the biofilm increased in the first hour, and then decreased. According to the previous studies, the concentration of *Shewanella* biofilm secreted riboflavin should increase over longer time periods, even until 72 hours. So it can be estimated that under the current experimental condition, the bacteria in the biofilm have stagnated after 1 hour. Future studies will be performed in a glove-box with N_2 to create a rigorous anaerobic environment, and a constant 30 °C to provide typical culture conditions. In addition, the calibration curve will be performed in the range of 1-5 μM in accordance with the concentration of biofilm secreted riboflavin and repeated at least 3 times.

X-scan and Approach Curve SECM experiments over masked biofilm strip showing evidence for riboflavin involved in Shewanella ET

SECM has the ability to scan over a substrate in the x-y direction, providing a spatial concentration profile of specific redox mediators over the target surface. The mechanism of mediator regeneration by cells or biofilms is complex and involves transmembrane ET. To investigate the pathway of the transmembrane ET reaction, SECM experiments were performed with various types of redox mediators. Figure **27** shows the results of a SECM x-scan over *Shewanella* biofilms in riboflavin and FcTMA redox mediator solution, respectively. All currents were normalized for comparison purposes. The x-scan data showed a sharper decrease current over the biofilm region in riboflavin than in FcTMA solution. When the tip was scanned horizontally above the biofilm in the presence of a redox mediator such as riboflavin, which can interact with the biofilm, the tip current above the cell was significantly lower than that above the glassy carbon. However, in FcTMA, the tip current decreased less dramatically, as it was in riboflavin when the tip was scanned horizontally above the biofilm. Both oxidized and reduced forms of riboflavin are neutral and can cross the cell membrane. Thus the sharp decrease in the current above biofilm is likely due to the consumption of riboflavin by the biofilm. Additionally, the current outside the biofilm in FcTMA was much steadier than that in riboflavin showing that there might be interactions between the biofilm edge with riboflavin.

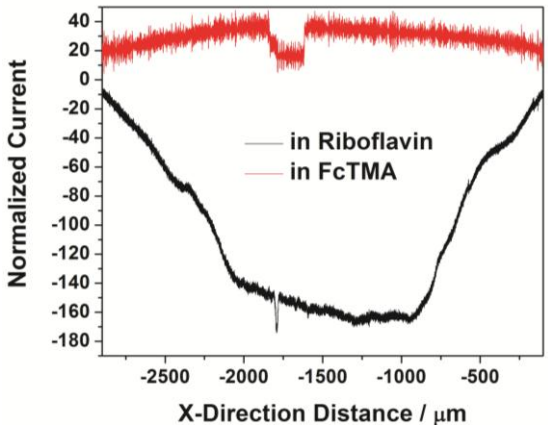

Figure 27. Normalized current changes of an SECM x-scan over masked *Shewanella* biofilm in riboflavin and FcTMA solution, respectively. Tip potential was held at -0.6 V in riboflavin and +0.6 V in FcTMA. All potentials are versus Ag/AgCl. The scan rate was 1.5 μm/s.

An SECM approach curve can be used to sense redox species concentration in the feedback over a biological substrate, and measure the local concentration of redox active molecules over a biofilm.[34] SECM is a powerful tool to measure both redox states of riboflavin in real-time by biasing the tip at -0.2 V (oxidizing at tip) and -0.6 V (reducing at tip). The biased potentials are based on the fact that the formal potential of riboflavin is -0.4 V vs. Ag/AgCl. Approach curves were collected over the biofilm. The approach curve of the oxidized riboflavin showed a steadily decrease current as the tip approached the biofilm, indicating a negative feedback of riboflavin oxidized form was found near the biofilm (Figure **28** red line). When the approach curves were collected under the reducing riboflavin condition, a sharper current drop was observed first as the tip moved closer to the biofilm, showing a negative deviation from the usual negative feedback mode approach curve as a result of consumption of mediator in the biofilm (Figure **28** black line). The approach curve data reveals that the concentration of reduced riboflavin decreased as the tip approached the biofilm but increased when the tip is really closed to the substrate surface, while a decrease steadily in the oxidized riboflavin.

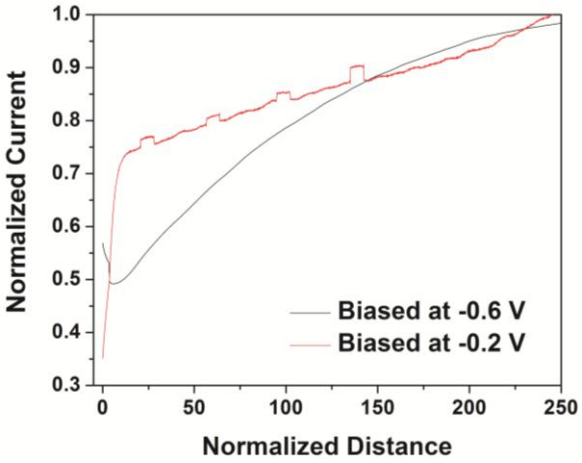

Figure 28. Approach curve represents of z-direction reduced and oxidized riboflavin over *Shewanella* biofilm. The tip was biased at -0.2 V (oxidizing potential) and -0.6 V (reducing potential), respectively. The approach rate was 1.5 μm/s.

CONCLUSIONS

This chapter is a preliminary study of *Shewanella* biofilm with SECM. More detailed studies need to be performed in the near future. However, with the results presented here, we are able to confirm that the soluble mediator that shuttle electron from bacterial interior to exterior involves riboflavin. In addition, SECM was able to offer real-time quantitative detection of the mediators secreted by *Shewanella*. Further research will study the direct ET pathway detection with SECM. Spatial resolution image with specific pathways will be carried out. Our research is going to offer a rapid and convenient evaluation method for extracellular ET detection. It has reconfirmed the assertion that electrons are shuttled among *Shewanella* biofilms. In addition, this study will facilitate the application of *Shewanella* species. More detailed studies about the secretion mechanism and shuttling will be performed in the future.

ACKNOWLEDGMENTS

The *S. oneidensis* MR-1 glycerol stock were received from Elliott group at Boston University. We really appreciate the help from Cynthia R. Mcnees from the Bachmann Lab at Vanderbilt University. She has taught us how to culture the cells, and performed LC-MS experiments in this work. We gratefully acknowledge the financial support from the National Science Foundation (DMR 0907619) and the NSF EPSCoR (EPS 10040083), and the Scialog Program from the Research Corporation for Science Advancement.

CHAPTER VII

CONCLUSIONS AND FUTURE SUGGESTIONS

RESEARCH SUMMARY

The results in this dissertation imply that the electrochemical studies of PSI can provide a deeper understanding of electron transfer (ET) properties of this photoactive protein found in abundance in nature. This understanding will drive expanding applications of this special protein for human utilization.

To study the ET behavior of PSI based system, a series of redox mediators have been investigated that includes inorganic complexes, organic compounds, and biological materials with formal potentials that span the potential difference of P700 and F_B for the first time. Our results show that the formal potential, oxidation state, absorbance, and concentration of the electrochemical mediator are all key factors that impact the photocurrent production. Additionally, the combination of redox mediators (such as methyl viologen /ferrocyanide) facilitates the biomimetic approach for the bio-hybrid system. This study provides invaluable insights into the properties that researchers should consider while choosing an appropriate mediator for an interest electrochemical system. In addition to use redox mediators to study PSI solar energy to electrical energy conversion properties, SECM has also been employed in this task. Photo responsive current has been simultaneously observed for both redox processes of PSI for the first time. Approach curves demonstrated that the ET of PSI in light conditions exhibited a limiting regeneration rate for the mediator. The SECM has also been utilized to interrogate the catalytic activity for hydrogen production of platinum particles which were photoreduced from platinum ions by PSI in a photocatalytic manner. This study demonstrated

the power of SECM to detect catalytic sites on a substrate surface, and also shows a promising future of building a higher efficiency fuel cell with platinum coupled PSI devices.

In summary, the electron transfer properties of PSI have been studied with redox mediators and SECM. The results showed that the selection of redox mediator as well as the control of electrode potential has profound effects on photocurrent production. In addition, the combination of PSI with platinum catalysts has been used to facilitate hydrogen production.

PERSPECTIVES, FUTURE DIRECTIONS AND RECOMMENDATIONS

As mentioned in the summary section and Chapter VI, the works in this dissertation have demonstrated the ability of natural materials such as PSI and *Shewanella* to convert solar energy or biomass into electricity or fuel. The potential and application of these materials must be explored further in order to meet our future energy requirements. From my research experience, the improvements can be carried out in the following areas: (1) exploit the function of SECM instrument for mechanism detection; (2) utilize PSI and *Shewanella* in novel configurations to extend their practical applications; (3) combine solar energy and biomass with fuel generation. To make these improvements, we need to learn from the nature and understand the design principles. The design target would be a complete system that is cheap, robust, and efficient. During the operation process a balance among the three targets and the optimization of the system are also necessary.

Fabrication of nanometer-sized tips to expand SECM studies

While all the SECM work carried out in this dissertation used ultramicroelectrodes (UMEs) in the micrometer size range, they brought significant advances in studies of fast heterogeneous reactions, and measurements in high resistant environments (i.e. *Shewanella* media). However, smaller UMEs,

in the nanometer size regime are needed to obtain higher resolution electrochemical images of the PSI structure (20-80 nm) and single *Shewanella* cells (0.2 -1.8 μm). PSI and *Shewanella* ET pathways involve even smaller nanometer-sized transient structures. To probe such structures, one needs a comparably sized electrode.[89] Thus, nanometer-sized electrodes are necessary. The advantages of using a UME with a smaller physical size include: (1) reduction in the current-resistance (iR) drop and double layer charging effects (2) providing higher resolution SECM images (3) allowing direct measurements in nanoliter volumes.[40] There are several fabrication methods of nanoelectrodes.[34, 89, 90] The most commonly employed processes involve the use of a laser puller. Detailed fabrication steps can be found in the sixth chapter of the Handbook of Electrochemistry edited by Zoski et al.[40]

With the nanoelectrodes, detection of the PSI orientation as a monolayer film should be possible. As predicted by the simulation results performed by Ceisielski *et al.*, most of the photocurrent produced by the PSI monolayer is negated by opposite orientation unless ~80% or more of the protein complexes are oriented in a similar configuration.[91] The immobilization methods that can orient PSI proteins would be an important approach to improve PSI photoresponse effectiveness. Researchers have tried to orient PSI on electrodes using a variety of methods from genetic modifications[92] to chemical modification of the surface[6, 14]. However it has been very difficult to actually test the orientation or the proteins on the surface. The closest attempts include the use of scanning tunneling spectroscopy to detect PSI orientation by measuring the current-rectification property,[6] and the employment of scanning near-field optical microscope to measure the PSI photocurrent.[93] Both of these methods, however, only allow one to analyze a single protein at a time. SECM is able to image an unlimited number of proteins in a single scan, depending only on

the size of the UME. Since PSI is a photodiode, using nanoelectrodes to scan over the protein complexes in the SECM image mode under illumination should detect the electrochemical gradients generated by the PSI reaction centers. The gradient information will depend on the activity of PSI reaction centers and the orientation of the proteins. This technique can be used in the screening of PSI immobilization methods for orientation.

With the help of nanometer-sized UMEs, single cell images of *Shewanella* would be possible. This could be used to determine how one pathway compares to another in real time, and visualize the spatial distribution of metal reduction (Mtr) cytochromes across the cell membrane. According to previous studies, the direct ET pathway involves the "Mtr" pathway, composed of three multiheme cytochromes (*mtrA, mtrC, cymA*) and an integral outer-membrane protein (*mtrB*), electrons are able to move from the menaquinone pool across the outer membrane through this channel.[83] Gene expression/deletion with different protein parts of *Shewanella* will help to determine the exact conductive components within *Shewanella* that allow for extracellular ET. Bretschger *et al.* showed that the overexpression of *mtrC* resulted in a 35% increase in current production.[94] Strains with deletion mutations for either of the cytochromes *MtrC* or *OmcA* apparently produce non-conductive nanowires, which may be an indication that functional nanowires are actually coated with *MtrC* and *OmcA*.[33, 95] The mutant strains could be compared with the wild type under the same cell culture condition using SECM nanoelectrodes to test these hypotheses.

Computational simulations for SECM mechanism studies

Analytical approximations are available only for a limited number of simple processes. However, the SECM theory for most systems is complicated and requires numerical solution of partial

differential equations, making it harder for an experimentalist to carry out quantitative SECM studies.[34] To exploit the reaction mechanisms, computational simulation would be necessary. Kinetic information about the rates of ET to the surface attached PSI can be obtained from SECM approach curves. Approach curves reflect the ability of the surface to rapidly transfer electrons as an UME tip approaches the surface. The amount of the feedback current can be used to measure the ET rate from the PSI reaction centers within the protein film. Chapter IV described the ET behavior of multilayer PSI films with SECM. To extend our understanding of the kinetics of this system, the geometry and the spatial distribution of the PSI reaction centers must be accurately described. Such a simulation could be very complicated and must be solved with commercial software package such as Comsol. The Comsol multiphysics software can also be employed to solve the rate constant based on the SECM approach curve results as performed by Xiong *et al.*[65]

SECM study of corrosion mechanisms

SECM is ideally suited to investigate the corrosion processes. It can provide information about insulating and conducting surfaces with high spatial resolution, and enable surface structural effects to be correlated with activity.[42] In addition, the tip can be used to initiate the reaction and to detect the corrosion products with the tip current providing quantitative information on the process. Wipf and Still have positioned the SECM tip close to a passivated iron surface and generated a local concentrations of the aggressive Cl^- ion to study corrosion effects.[96] *Shewanella* is included in the category of dissimilatory metal reduction bacteria and is able to reduce Fe (III) to Fe (II) and act as an important component in the biogeochemical recycling of iron on the earth.[97] Iron is the fourth most abundant element on Earth and is an essential trace metal in nearly all organisms. By reducing ferric iron compounds, dissimilatory metal reducers function in a key role in the global iron cycle

by affecting the bioavailability of soluble iron for other organisms.[98, 99] SECM can be used in the study of corrosion mechanism for *Shewanella* Fe(III)-respiring bacteria.

Integrate PSI into flexible materials

The research performed by our group showed that PSI modified p-doped silicon was able to generate 875 $\mu A/cm^2$ photocurrent density.[53] This makes the utilization of PSI for daily human needs very promising. Besides the integration of PSI on solid materials such as metals or semiconductors, flexible materials such as conductive polymers, electronic textile may be explored as the substrate. The advantages of flexible materials include portability, light-weight, and space-saving. The Rogner group in Germany is working on the immobilization of PSI within an Os complex containing redox polymer as matrix and electron donor for PSI.[20, 50] It is important to design the PSI immobilization within a polymer matrix such that once the electrons holes are injected into the polymer they do not recombine with one of the holes generated by another PSI protein. Additionally, the migration of the charge carriers needs to be facilitated.

Besides the development of novel substrate matrixes for PSI energy utilization, the configuration and arrangement for massive energy storage units should also be considered. To get optimal light absorption and minimal shading from the top branches down, PSI can be assembled on to flexible materials with highly branched structures, like leaves arranged on trees (i.e. pine trees). The Fibonacci series arrangement of branches favors optimum light absorption. There was an experiment performed by Aidan Dwyer, who used phyllotaxis — the way leaves are arranged on plant stems in nature — as inspiration to arrange an array of solar panels in a way that generates 20-50% more energy than a uniform, flat panel array.[100]

Combine PSI with Hydrogenase and PSII in fuel application

If solar energy can be used to split water molecules to produce hydrogen, it could be used as an abundant material to generate energy-rich fuel to produce electricity and other domestic applications. This technology would then be capable of supplying a substantial portion of global energy demand. The key of this technology is to discover inexpensive catalysts to achieve fast reaction rate under mild conditions. One strategy is to use natural systems as blueprint for either the design of appropriately modified natural systems or for the construction of semi-artificial model systems.[101] Among the energy converting processes in nature, light-driven water splitting photosynthesis of plants is the best model.

PSI allows an unsurpassed efficient light-induced charge separation, and its F_B-site has a formal potential ($E^{0\prime}$= - 580 mV vs. NHE[16]) can provide high driving force for H^+ reduction (~ -250 mV vs. NHE[102]). However, as PSI is not capable of reducing protons at the Fe-S cluster, a proton reducing catalyst has to be electrically connected to the acceptor site of PSI.[20] Although the results in Chapter V show that photo-precipitated platinum on PSI films is able to generate hydrogen, the replacement of platinum with biological materials would be valuable due to the high price and the limited availability on the earth. Krassen *et al.* has demonstrated how PSI can be integrated with hydrogenase in an electrochemical device for hydrogen production.[103] This has provided a significant step toward the development of environmentally acceptable regenerative systems for hydrogen production.

Currently, hydrogen production has not been combined with photo-driving water splitting natural materials. PSII is one of the most famous enzymes for light-driven water splitting in mild condition. It would be favorable to integrate PSII and PSI-hydrogenase artificially into bioelectrochemical devices for fuel production. However, water oxidation and proton reduction processes have to be

designed in spatially separated manners. If the products (i.e. hydrogen and oxygen from water) are not separated from each other, the system may short circuit and products could recombine. Permeable membrane could be utilized for the separation purpose.

Utilization of Shewanella in microbial fuel cells

Microbial fuel cells (MFCs) are electrochemical devices that incorporate microbial organisms (microbes) into the design in order to produce electricity through the biologically catalyzed oxidation of soluble, electron donating substrate.[104, 105] MFCs are an important fuel cell type in solving energy crisis problems. *Shewanella* can be used in the mediatorless MFC technique, which utilizes microbes that can form direct contacts between their cellular apparatus and the anode surface.[106] Mediatorless MFCs are suitable for *Shewanella* because of their ability to reduce external metals and ability to form an efficient pathway for electrons generated from metabolism to an extracellular material.[107]

Future for Redox Mediators

As described in Chapter III, the PSI-based system relies predominantly on redox active mediators to transport electrons through the electrolyte. In addition, the results also suggest that the selection of mediator play important roles in the enhancement of the system performance. Although the results in Chapter III show that ferricyanide generates the largest photocurrent in the gold-based PSI system, the mediator that generated the highest photocurrent in the p-doped silicon was methyl viologen. These phenomena suggest that different systems require different mediators. In order to further optimize the efficiency more redox mediators with different E^0 to match F_B/P700 as well as the immobilization substrate should be analyzed. The candidates for these mediator studies can be found in the mediator compilation performed by Fultz *et al*.[22] Moreover, different groups of redox

mediator mixtures should be performed. Except the equal molar mixture of mediators, different concentration ratio between electron donors and acceptors should also be tried. We hypothesize that if an electron donor is used along with an electron acceptor with the appropriate formal potential the PSI reaction centers can be regenerated continually. Lastly, redox mediators with proper E^0 and light absorbance can be synthesized artificially. Mershin *et al.* synthesized Co(II)/Co(III) ion-containing electrolyte to play the role of plastocyanin, and a ZnO-nanowire to replace ferredoxin in a biophotovoltaic solar cell, generating encouraging results.[108] The synthesis target could refer to nature redox couple (i.e. plastocyanin and ferredoxin) to make the mediators diffuse effectively into the PSI docking pocket. The key is to obtain a balance between the maximum electrochemical voltages with the speed of the electron transfer out of PSI.

CONCLUSIONS

The ability of converting solar energy to electricity and combining catalysis for hydrogen production makes PSI one of the most promising materials to study in alternative energy. On the other hand, the ability of reducing toxic metals in waste water and to be integrated in microbial fuel cells has made *Shewanella* as one of the most interesting study candidates in environmental science. PSI and *Shewanella* are promising natural materials that can be used to help solve the energy crisis and environmental pollution problems. Finally, these studies have broadened the application of SECM in biological and alternative energy fields.

REFERENCES

1. Administration, U. S. E. I. Annual Energy Review 2011. http://www.eia.gov/aer.

2. Chitnis, P. R., PHOTOSYSTEM I: Function and Physiology. *Annu. Rev. Plant Physiol.* **2001,** *52*, 593-626.

3. Nelson, N.; Yocum, C. F., Structure and function of photosystems I and II. *Annu. Rev. Plant Biol.* **2006,** *57*, 521-65.

4. Amunts, A.; Toporik, H.; Borovikova, A.; Nelson, N., Structure determination and improved model of plant photosystem I. *J. Biol. Chem.* **2010,** *285* (5), 3478-86.

5. Greenbaum, E., Platinized Chloroplasts - a Novel Photocatalytic Material. *Science* **1985,** *230* (4732), 1373-1375.

6. Lee, I.; Lee, J. W.; Greenbaum, E., Biomolecular electronics: Vectorial arrays of photosynthetic reaction centers. *Phys. Rev. Lett.* **1997,** *79* (17), 3294-3297.

7. Das, R.; Kiley, P. J.; Segal, M.; Norville, J.; Yu, A. A.; Wang, L. Y.; Trammell, S. A.; Reddick, L. E.; Kumar, R.; Stellacci, F.; Lebedev, N.; Schnur, J.; Bruce, B. D.; Zhang, S. G.; Baldo, M., Integration of photosynthetic protein molecular complexes in solid-state electronic devices. *Nano Lett.* **2004,** *4* (6), 1079-1083.

8. Terasaki, N.; Yamamoto, N.; Hiraga, T.; Sato, I.; Inoue, Y.; Yamada, S., Fabrication of novel photosystem I-gold nanoparticle hybrids and their photocurrent enhancement. *Thin Solid Films* **2006,** *499* (1-2), 153-156.

9. Terasaki, N.; Yamamoto, N.; Tamada, K.; Hattori, M.; Hiraga, T.; Tohri, A.; Sato, I.; Iwai, M.; Iwai, M.; Taguchi, S.; Enami, I.; Inoue, Y.; Yamanoi, Y.; Yonezawa, T.; Mizuno, K.; Murata, M.; Nishihara, H.; Yoneyama, S.; Minakata, M.; Ohmori, T.; Sakai, M.; Fujii, M., Bio-photo sensor: Cyanobacterial photosystem I coupled with transistor via molecular wire. *biochim biophys acta.* **2007,** *1767* (6), 653-659.

10. Frolov, L.; Rosenwaks, Y.; Carmeli, C.; Carmeli, I., Fabrication of a photoelectronic device by direct chemical binding of the photosynthetic reaction center protein to metal surfaces. *Adv. Mater.* **2005,** *17* (20), 2434-2437.

11. Carmeli, I.; Frolov, L.; Carmeli, C.; Richter, S., Photovoltaic activity of photosystem I-based self-assembled monolayer. *J. Am. Chem. Soc.* **2007,** *129* (41), 12352-12353.

12. Proux-Delrouyre, V.; Demaille, C.; Leibl, W.; Setif, P.; Bottin, H.; Bourdillon, C., Electrocatalytic investigation of light-induced electron transfer between cytochrome c(6) and photosystem I. *J. Am. Chem. Soc.* **2003,** *125* (45), 13686-13692.

13. Munge, B.; Das, S. K.; Ilagan, R.; Pendon, Z.; Yang, J.; Frank, H. A.; Rusling, J. F., Electron transfer reactions of redox cofactors in spinach Photosystem I reaction center protein in lipid films on electrodes. *J. Am. Chem. Soc.* **2003,** *125* (41), 12457-12463.

14. Ko, B. S.; Babcock, B.; Jennings, G. K.; Tilden, S. G.; Peterson, R. R.; Cliffel, D.; Greenbaum, E., Effect of surface composition on the adsorption of photosystem I onto alkanethiolate self-assembled monolayers on gold. *Langmuir* **2004,** *20* (10), 4033-4038.

15. Ciobanu, M.; Kincaid, H. A.; Jennings, G. K.; Cliffel, D. E., Photosystem I patterning imaged by scanning electrochemical microscopy. *Langmuir* **2005,** *21* (2), 692-628.

16. Ciobanu, M.; Kincaid, H. A.; Lo, V.; Dukes, A. D.; Jennings, G. K.; Cliffel, D. E., Electrochemistry and photoelectrochemistry of photosystem I adsorbed on hydroxyl-terminated monolayers. *J. Electroanal. Chem.* **2007,** *599* (1), 72-78.

17. Faulkner, C. J.; Lees, S.; Ciesielski, P. N.; Cliffel, D. E.; Jennings, G. K., Rapid assembly of photosystem I monolayers on gold electrodes. *Langmuir* **2008,** *24* (16), 8409-8412.

18. Ciesielski, P. N.; Hijazi, F. M.; Scott, A. M.; Faulkner, C. J.; Beard, L.; Emmett, K.; Rosenthal, S. J.; Cliffel, D.; Jennings, G. K., Photosystem I - Based biohybrid photoelectrochemical cells. *Bioresour. Technol.* **2010,** *101* (9), 3047-3053.

19. Ciesielski, P. N.; Faulkner, C. J.; Irwin, M. T.; Gregory, J. M.; Tolk, N. H.; Cliffel, D. E.; Jennings, G. K., Enhanced Photocurrent Production by Photosystem I Multilayer Assemblies. *Adv. Funct. Mater.* **2010,** *20* (23), 4048-4054.

20. Badura, A.; Kothe, T.; Schuhmann, W.; Rogner, M., Wiring photosynthetic enzymes to electrodes. *Energy Environ. Sci.* **2011,** *4* (9), 3263-3274.

21. Szentrimay, R.; Yeh, P.; Kuwana, T., Evaluation of Mediator-Titrants for the Indirect Coulometric Titration of Biocomponents. In *Electrochemical Studies of Biological Systems*, AMERICAN CHEMICAL SOCIETY: 1977; Vol. 38, pp 143-169.

22. Fultz, M. L.; Durst, R. A., Mediator compounds for the electrochemical study of biological redox systems: a compilation. *Anal. Chim. Acta* **1982,** *140* (1), 1-18.

23. Venkateswaran, K.; Moser, D. P.; Dollhopf, M. E.; Lies, D. P.; Saffarini, D. A.; MacGregor, B. J.; Ringelberg, D. B.; White, D. C.; Nishijima, M.; Sano, H.; Burghardt, J.; Stackebrandt, E.; Nealson, K. H., Polyphasic taxonomy of the genus Shewanella and description of Shewanella oneidensis sp. nov. *Int J Syst Bacteriol* **1999,** *49 Pt 2*, 705-24.

24. Stenstrom, I. M.; Molin, G., Classification of the spoilage flora of fish, with special reference to Shewanella putrefaciens. *J Appl Bacteriol* **1990,** *68* (6), 601-18.

25. Hau, H. H.; Gralnick, J. A., Ecology and biotechnology of the genus Shewanella. *Annu. Rev. Microbiol.* **2007,** *61*, 237-58.

26. Myers, C. R.; Nealson, K. H., Bacterial manganese reduction and growth with manganese oxide as the sole electron acceptor. *Science* **1988,** *240* (4857), 1319-21.

27. Lovley, D. R., Bioremediation of organic and metal contaminants with dissimilatory metal reduction. *J Ind Microbiol* **1995,** *14* (2), 85-93.

28. Elias, D. A.; Krumholz, L. R.; Wong, D.; Long, P. E.; Suflita, J. M., Characterization of microbial activities and U reduction in a shallow aquifer contaminated by uranium mill tailings. *Microbial Ecology* **2003,** *46* (1), 83-91.

29. Nevin, K. P.; Lovley, D. R., Mechanisms for accessing insoluble Fe(III) oxide during dissimilatory Fe(III) reduction by Geothrix fermentans. *Appl. Environ. Microbiol.* **2002,** *68* (5), 2294-9.

30. Lies, D. P.; Hernandez, M. E.; Kappler, A.; Mielke, R. E.; Gralnick, J. A.; Newman, D. K., Shewanella oneidensis MR-1 uses overlapping pathways for iron reduction at a distance and by direct contact under conditions relevant for Biofilms. *Appl. Environ. Microbiol.* **2005,** *71* (8), 4414-26.

31. Marsili, E.; Baron, D. B.; Shikhare, I. D.; Coursolle, D.; Gralnick, J. A.; Bond, D. R., Shewanella secretes flavins that mediate extracellular electron transfer. *Proc. Natl. Acad. Sci. U. S. A.* **2008,** *105* (10), 3968-73.

32. Jiang, X.; Hu, J.; Fitzgerald, L. A.; Biffinger, J. C.; Xie, P.; Ringeisen, B. R.; Lieber, C. M., Probing electron transfer mechanisms in Shewanella oneidensis MR-1 using a nanoelectrode platform and single-cell imaging. *Proc. Natl. Acad. Sci. U. S. A.* **2010,** *107* (39), 16806-10.

33. Brutinel, E. D.; Gralnick, J. A., Shuttling happens: soluble flavin mediators of extracellular electron transfer in Shewanella. *Appl. Microbiol. Biotechnol.* **2012,** *93* (1), 41-48.

34. Bard, A. J.; Mirkin, M. V., *Scanning electrochemical microscopy*. Marcel Dekker: New York, 2001; p x, 650 p.

35. Rozkiewicz, D. I.; Ravoo, B. J.; Reinhoudt, D. N., Reversible covalent patterning of self-assembled monolayers on gold and silicon oxide surfaces. *Langmuir* **2005,** *21* (14), 6337-6343.

36. Reeves, S. G.; Hall, D. O.; Anthony San, P., [8] Higher plant chloroplasts and grana: General preparative procedures (excluding high carbon dioxide fixation ability chloroplasts). In *Methods Enzymol.*, Academic Press: 1980; Vol. Volume 69, pp 85-94.

37. Baba, K.; Itoh, S.; Hastings, G.; Hoshina, S., Photoinhibition of Photosystem I electron transfer activity in isolated Photosystem I preparations with different chlorophyll contents. *Photosynth. Res.* **1996,** *47* (2), 121-130.

38. Porra, R., The chequered history of the development and use of simultaneous equations for the accurate determination of chlorophylls a and b. *Photosynth. Res.* **2002,** *73* (1), 149-156.

39. Bard, A. J.; Faulkner, L. R., *Electrochemical methods : fundamentals and applications*. 2nd ed.; Wiley: New York, 2001; p 833 p.

40. Zoski, C. G., *Handbook of electrochemistry*. Elsevier: Amsterdam; Boston, 2007.

41. Sun, P.; Laforge, F. O.; Mirkin, M. V., Scanning electrochemical microscopy in the 21st century. *Phys. Chem. Chem. Phys.* **2007,** *9* (7), 802-823.

42. Kwak, J.; Bard, A. J., Scanning Electrochemical Microscopy - Theory of the Feedback Mode. *Analytical Chemistry* **1989,** *61* (11), 1221-1227.

43. Brundle, C. R.; Evans, C. A., Jr.; Wilson, S., Encyclopedia of Materials Characterization - Surfaces, Interfaces, Thin Films. Elsevier: 1992.

44. Hillig, K. W., Principles of Instrumental Analysis, 2nd Edition - Skoog,Da, West,Dm. *J. Am. Chem. Soc.* **1984,** *106* (5), 1536-1536.

45. Frolov, L.; Rosenwaks, Y.; Carmeli, C.; Carmeli, I., Fabrication of a photoelectronic device by direct chemical binding of the photosynthetic reaction center protein to metal surfaces. *Adv. Mater. (Weinheim, Ger.)* **2005,** *17* (20), 2434-+.

46. Brettel, K.; Leibl, W., Electron transfer in photosystem I. *Biochim. Biophys. Acta, Bioenerg.* **2001,** *1507* (1-3), 100-114.

47. Terasaki, N.; Yamamoto, N.; Tamada, K.; Hattori, M.; Hiraga, T.; Tohri, A.; Sato, I.; Iwai, M.; Iwai, M.; Taguchi, S.; Enami, I.; Inoue, Y.; Yamanoi, Y.; Yonezawa, T.; Mizuno, K.; Murata, M.; Nishihara, H.; Yoneyama, S.; Minakata, M.; Ohmori, T.; Sakai, M.; Fujii, M., Bio-photo sensor: Cyanobacterial photosystem I coupled with transistor via molecular wire. *Biochim. Biophys. Acta* **2007,** *1767* (6), 653-659.

48. Ciesielski, P. N.; Scott, A. M.; Faulkner, C. J.; Berron, B. J.; Cliffel, D. E.; Jennings, G. K., Functionalized Nanoporous Gold Leaf Electrode Films for the Immobilization of Photosystem I. *ACS Nano* **2008,** *2* (12), 2465-2472.

49. Lee, J. W.; Lee, I.; Laible, P. D.; Owens, T. G.; Greenbaum, E., Chemical Platinization and Its Effect on Excitation Transfer Dynamics and P700 Photooxidation Kinetics in Isolated Photosystem-I. *Biophys. J.* **1995,** *69* (2), 652-659.

50. Badura, A.; Guschin, D.; Kothe, T.; Kopczak, M. J.; Schuhmann, W.; Rogner, M., Photocurrent generation by photosystem 1 integrated in crosslinked redox hydrogels. *Energy Environ. Sci.* **2011,** *4* (7), 2435-2440.

51. LeBlanc, G.; Chen, G.; Gizzie, E. A.; Jennings, G. K.; Cliffel, D. E., Enhanced Photocurrents of Photosystem I Films on p-Doped Silicon. *Adv Mater* **2012,** *DOI:10.1002/adma.201202794*

52. Forouzan, F.; Bard, A. J.; Mirkin, M. V., Voltammetric and scanning electrochemical microscopic studies of the adsorption kinetics and self-assembly of n-alkanethiol monolayers on gold. *Isr. J. Chem.* **1997,** *37* (2-3), 155-163.

53. Leblanc, G.; Chen, G.; Gizzie, E. A.; Jennings, G. K.; Cliffel, D. E., Enhanced Photocurrents of Photosystem I Films on p-Doped Silicon. *Adv Mater* **2012,** *24* (44), 5959-62.

54. Kennis, J. T. M.; Gobets, B.; van Stokkum, I. H. M.; Dekker, J. P.; van Grondelle, R.; Fleming, G. R., Light harvesting by chlorophylls and carotenoids in the photosystem I core complex of Synechococcus elongatus: A fluorescence upconversion study. *J. Phys. Chem. B* **2001,** *105* (19), 4485-4494.

55. Terasaki, N.; Yamamoto, N.; Hiraga, T.; Yamanoi, Y.; Yonezawa, T.; Nishihara, H.; Ohmori, T.; Sakai, M.; Fujii, M.; Tohri, A.; Iwai, M.; Inoue, Y.; Yoneyama, S.; Minakata, M.; Enami, I., Plugging a molecular wire into photosystem I: reconstitution of the photoelectric conversion system on a gold electrode. *Angew. Chem., Int. Ed. Engl.* **2009,** *48* (9), 1585-7.

56. Yehezkeli, O.; Wilner, O. I.; Tel-Vered, R.; Roizman-Sade, D.; Nechushtai, R.; Willner, I., Generation of Photocurrents by Bis-aniline-Cross-Linked Pt Nanoparticle/Photosystem I Composites on Electrodes. *J. Phys. Chem. B* **2010,** *114* (45), 14383-14388.

57. Vuorilehto, K., Stable, colourless and water-soluble electron-transfer mediators used in enzyme electrochemistry. *J. Appl. Electrochem.* **2008,** *38* (10), 1427-1433.

58. Terasaki, N.; Yamamoto, N.; Hattori, M.; Tanigaki, N.; Hiraga, T.; Ito, K.; Konno, M.; Iwai, M.; Inoue, Y.; Uno, S.; Nakazato, K., Photosensor based on an FET utilizing a biocomponent of photosystem I for use in imaging devices. *Langmuir* **2009,** *25* (19), 11969-74.

59. Bard, A. J.; Faulkner, L. R., *Electrochemical methods : fundamentals and applications*. 2nd ed.; Wiley: New York, 2001.

60. Bard, A. J.; Fan, F. R.; Pierce, D. T.; Unwin, P. R.; Wipf, D. O.; Zhou, F., Chemical imaging of surfaces with the scanning electrochemical microscope. *Science* **1991,** *254* (5028), 68-74.

61. Tsionsky, M.; Cardon, Z. G.; Bard, A. J.; Jackson, R. B., Photosynthetic Electron Transport in Single Guard Cells as Measured by Scanning Electrochemical Microscopy. *Plant Physiol.* **1997,** *113* (3), 895-901.

62. Parthasarathy, M.; Singh, S.; Hazra, S.; Pillai, V. K., Imaging the stomatal physiology of somatic embryo-derived peanut leaves by scanning electrochemical microscopy. *Anal. Bioanal. Chem.* **2008,** *391* (6), 2227-33.

63. Flexer, V.; Mano, N., From Dynamic Measurements of, Photosynthesis in a Living Plant to Sunlight Transformation into Electricity. *Anal. Chem.* **2010,** *82* (4), 1444-1449.

64. Yasukawa, T.; Kaya, T.; Matsue, T., Imaging of photosynthetic and respiratory activities of a single algal protoplast by scanning electrochemical microscopy. *Chem. Lett.* **1999,** (9), 975-976.

65. Xiong, H.; Guo, J. D.; Amemiya, S., Probing heterogeneous electron transfer at an unbiased conductor by scanning electrochemical microscopy in the feedback mode. *Anal. Chem.* **2007,** *79* (7), 2735-2744.

66. Tefashe, U. M.; Nonomura, K.; Vlachopoulos, N.; Hagfeldt, A.; Wittstock, G., Effect of Cation on Dye Regeneration Kinetics of N719-Sensitized TiO2 Films in Acetonitrile-Based and Ionic-Liquid-Based Electrolytes Investigated by Scanning Electrochemical Microscopy. *J. Phys. Chem. C* **2012,** *116* (6), 4316-4323.

67. Lipkowski, J.; Ross, P. N., *Electrocatalysis*. Wiley-VCH: New York, 1998; p xiv, 376 p.

68. Utschig, L. M.; Dimitrijevic, N. M.; Poluektov, O. G.; Chemerisov, S. D.; Mulfort, K. L.; Tiede, D. M., Photocatalytic Hydrogen Production from Noncovalent Biohybrid Photosystem I/Pt Nanoparticle Complexes. *Journal of Physical Chemistry Letters* **2011,** *2* (3), 236-241.

69. Evans, B. R.; O'Neill, H. M.; Hutchens, S. A.; Bruce, B. D.; Greenbaum, E., Enhanced photocatalytic hydrogen evolution by covalent attachment of plastocyanin to photosystem I. *Nano Lett.* **2004,** *4* (10), 1815-1819.

70. Grimme, R. A.; Lubner, C. E.; Bryant, D. A.; Golbeck, J. H., Photosystem I/molecular wire/metal nanoparticle bioconjugates for the photocatalytic production of H-2. *J. Am. Chem. Soc.* **2008,** *130* (20), 6308-+.

71. Iwuchukwu, I. J.; Vaughn, M.; Myers, N.; O'Neill, H.; Frymier, P.; Bruce, B. D., Self-organized photosynthetic nanoparticle for cell-free hydrogen production. *Nat. Nanotechnol.* **2010,** *5* (1), 73-79.

72. Grimme, R. A.; Lubner, C. E.; Golbeck, J. H., Maximizing H-2 production in Photosystem I/dithiol molecular wire/platinum nanoparticle bioconjugates. *Dalton Trans.* **2009,** (45), 10106-10113.

73. LeBlanc, G.; Chen, G. P.; Jennings, G. K.; Cliffel, D. E., Photoreduction of Catalytic Platinum Particles Using Immobilized Multilayers of Photosystem I. *Langmuir* **2012,** *28* (21), 7952-7956.

74. Zhou, J. F.; Zu, Y. B.; Bard, A. J., Scanning electrochemical microscopy Part 39. The proton/hydrogen mediator system and its application to the study of the electrocatalysis of hydrogen oxidation. *J. Electroanal. Chem.* **2000,** *491* (1-2), 22-29.

75. Lovley, D. R., The microbe electric: conversion of organic matter to electricity. *Curr. Opin. Biotechnol.* **2008,** *19* (6), 564-571.

76. Rabaey, K.; Rozendal, R. A., Microbial electrosynthesis - revisiting the electrical route for microbial production. *Nat. Rev. Microbiol.* **2010,** *8* (10), 706-716.

77. Ross, D. E.; Flynn, J. M.; Baron, D. B.; Gralnick, J. A.; Bond, D. R., Towards Electrosynthesis in Shewanella: Energetics of Reversing the Mtr Pathway for Reductive Metabolism. *PLoS One* **2011,** *6* (2).

78. Gray, H. B.; Winkler, J. R., Electron transfer in proteins. *Annu. Rev. Biochem.* **1996,** *65*, 537-561.

79. Freire, R. S.; Pessoa, C. A.; Mello, L. D.; Kubota, L. T., Direct electron transfer: An approach for electrochemical biosensors with higher selectivity and sensitivity. *J. Braz. Chem. Soc.* **2003,** *14* (2), 230-243.

80. Gorton, L.; Lindgren, A.; Larsson, T.; Munteanu, F. D.; Ruzgas, T.; Gazaryan, I., Direct electron transfer between heme-containing enzymes and electrodes as basis for third generation biosensors. *Anal. Chim. Acta* **1999,** *400*, 91-108.

81. Hernandez, M. E.; Newman, D. K., Extracellular electron transfer. *Cell. Mol. Life Sci.* **2001,** *58* (11), 1562-1571.

82. Gralnick, J. A.; Newman, D. K., Extracellular respiration. *Mol. Microbiol.* **2007,** *65* (1), 1-11.

83. Shi, L.; Squier, T. C.; Zachara, J. M.; Fredrickson, J. K., Respiration of metal (hydr)oxides by Shewanella and Geobacter: a key role for multihaem c-type cytochromes. *Mol. Microbiol.* **2007,** *65* (1), 12-20.

84. Okamoto, A.; Nakamura, R.; Hashimoto, K., In-vivo identification of direct electron transfer from Shewanella oneidensis MR-1 to electrodes via outer-membrane OmcA-MtrCAB protein complexes. *Electrochim. Acta* **2011,** *56* (16), 5526-5531.

85. Costerton, J. W.; Stewart, P. S.; Greenberg, E. P., Bacterial Biofilms: A Common Cause of Persistent Infections. *Science* **1999,** *284* (5418), 1318-1322.

86. Stewart, P. S.; Franklin, M. J., Physiological heterogeneity in biofilms. *Nat. Rev. Microbiol.* **2008,** *6* (3), 199-210.

87. Xu, K. D.; Stewart, P. S.; Xia, F.; Huang, C. T.; McFeters, G. A., Spatial physiological heterogeneity in Pseudomonas aeruginosa biofilm is determined by oxygen availability. *Appl. Environ. Microbiol.* **1998,** *64* (10), 4035-4039.

88. Albert, A., The metal-binding properties of riboflavin. *Biochem. J.* **1950,** *47* (3), xxvii.

89. Shao, Y. H.; Mirkin, M. V.; Fish, G.; Kokotov, S.; Palanker, D.; Lewis, A., Nanometer-sized electrochemical sensors. *Anal. Chem.* **1997,** *69* (8), 1627-1634.

90. Katemann, B. B.; Schuhmann, T., Fabrication and characterization of needle-type Pt-disk nanoelectrodes. *Electroanalysis* **2002,** *14* (1), 22-28.

91. Ciesielski, P. N.; Cliffel, D. E.; Jennings, G. K., Kinetic Model of the Photocatalytic Effect of a Photosystem I Monolayer on a Planar Electrode Surface. *J. Phys. Chem. A* **2011,** *115* (15), 3326-3334.

92. Carmeli, I.; Mangold, M.; Frolov, L.; Zebli, B.; Carmeli, C.; Richter, S.; Holleitner, A. W., A photosynthetic reaction center covalently bound to carbon nanotubes. *Adv. Mater. (Weinheim, Ger.)* **2007,** *19* (22), 3901-+.

93. Gerster, D.; Reichert, J.; Bi, H.; Barth, J. V.; Kaniber, S. M.; Holleitner, A. W.; Visoly-Fisher, I.; Sergani, S.; Carmeli, I., Photocurrent of a single photosynthetic protein. *Nat. Nanotechnol.* **2012,** *7* (10), 673-676.

94. Bretschger, O.; Obraztsova, A.; Sturm, C. A.; Chang, I. S.; Gorby, Y. A.; Reed, S. B.; Culley, D. E.; Reardon, C. L.; Barua, S.; Romine, M. F.; Zhou, J.; Beliaev, A. S.; Bouhenni, R.; Saffarini, D.; Mansfeld, F.; Kim, B. H.; Fredrickson, J. K.; Nealson, K. H., Current production and metal oxide reduction by Shewanella oneidensis MR-1 wild type and mutants. *Appl. Environ. Microbiol.* **2007,** *73* (21), 7003-7012.

95. Gorby, Y. A.; Yanina, S.; McLean, J. S.; Rosso, K. M.; Moyles, D.; Dohnalkova, A.; Beveridge, T. J.; Chang, I. S.; Kim, B. H.; Kim, K. S.; Culley, D. E.; Reed, S. B.; Romine, M. F.; Saffarini, D. A.; Hill, E. A.; Shi, L.; Elias, D. A.; Kennedy, D. W.; Pinchuk, G.; Watanabe, K.; Ishii, S.; Logan, B.; Nealson, K. H.; Fredrickson, J. K., Electrically conductive bacterial nanowires produced by Shewanella oneidensis strain MR-1 and other microorganisms. *Proc. Natl. Acad. Sci. U. S. A.* **2006,** *103* (30), 11358-63.

96. Still, J. W.; Wipf, D. O., Breakdown of the iron passive layer by use of the scanning electrochemical microscope. *J. Electrochem. Soc.* **1997,** *144* (8), 2657-2665.

97. Lovley, D. R., Dissimilatory Fe(III) and Mn(IV) reduction. *Microbiol Rev* **1991,** *55* (2), 259-87.

98. Nealson, K. H.; Saffarini, D., Iron and manganese in anaerobic respiration: environmental significance, physiology, and regulation. *Annu. Rev. Microbiol.* **1994,** *48*, 311-43.

99. Weber, K. A.; Achenbach, L. A.; Coates, J. D., Microorganisms pumping iron: anaerobic microbial iron oxidation and reduction. *Nat. Rev. Microbiol.* **2006,** *4* (10), 752-764.

100. Michler, A. 13-Year-Old Makes Solar Power Breakthrough by Harnessing the Fibonacci Sequence http://inhabitat.com/13-year-old-makes-solar-power-breakthrough-by-harnessing-the-fibonacci-sequence/.

101. Badura, A.; Esper, B.; Ataka, K.; Grunwald, C.; Woll, C.; Kuhlmann, J.; Heberle, J.; Rogner, M., Light-driven water splitting for (bio-)hydrogen production: photosystern 2 as the central part of a bioelectrochemical device. *Photochem. Photobiol.* **2006,** *82* (5), 1385-1390.

102. Vincent, K. A.; Parkin, A.; Armstrong, F. A., Investigating and exploiting the electrocatalytic properties of hydrogenases. *Chem. Rev. (Washington, DC, U. S.)* **2007,** *107* (10), 4366-4413.

103. Krassen, H.; Schwarze, A.; Friedrich, B.; Ataka, K.; Lenz, O.; Heberle, J., Photosynthetic Hydrogen Production by a Hybrid Complex of Photosystem I and [NiFe]-Hydrogenase. *ACS Nano* **2009,** *3* (12), 4055-4061.

104. Bullen, R. A.; Arnot, T. C.; Lakeman, J. B.; Walsh, F. C., Biofuel cells and their development. *Biosens. Bioelectron.* **2006,** *21* (11), 2015-2045.

105. Lovley, D. R., Microbial fuel cells: novel microbial physiologies and engineering approaches. *Curr. Opin. Biotechnol.* **2006,** *17* (3), 327-332.

106. Chaudhuri, S. K.; Lovley, D. R., Electricity generation by direct oxidation of glucose in mediatorless microbial fuel cells. *Nat. Biotechnol.* **2003,** *21* (10), 1229-1232.

107. Heilmann, J.; Logan, B. E., Production of electricity from proteins using a microbial fuel cell. *Water Environ. Res.* **2006,** *78* (5), 531-537.

108. Mershin, A.; Matsumoto, K.; Kaiser, L.; Yu, D. Y.; Vaughn, M.; Nazeeruddin, M. K.; Bruce, B. D.; Graetzel, M.; Zhang, S. G., Self-assembled photosystem-I biophotovoltaics on nanostructured TiO2 and ZnO. *Scientific Reports* **2012,** *2*, 1-6.

Gongping Chen - Curriculum Vitae

Department of Chemistry
Vanderbilt University
7330 Stevenson Center

Nashville, TN 37235
gongping.chen@vanderbilt.edu
615-594-6434

Education

08/2008-Present Ph.D. in Analytical Chemistry, Vanderbilt University, May 2013

09/2001-06/2005 B.S. in Applied Chemistry, Nanjing University, China

Professional Experience

2009-Present **Research Assistant, Vanderbilt University**

Advisor: Dr. David E. Cliffel

Study redox mediator systems for Photosystem I (PSI) multilayer films

Study electrochemical and photoelectrochemical behavior of PSI with scanning electrochemical microscopy (SECM)

Image catalytic activity of platinized PSI for hydrogen reduction by SECM.

Investigation of the dissimilatory metal reduction pathways of *Shewanella* with spatial resolution

07/2012-10/2012 **Research Intern, Prinston Pharmaceutical Inc. (New Jersey)**

Implemented dissolution tests and assay tests for new formulations of generic drugs in Department of Analytical

2008-2009 **Teaching Assistant, Vanderbilt University**

Instructed sections of 24 students in the general chemistry lab

08/2005-08/2008 **Chemist, Arch Chemicals (China, Suzhou) Co., Ltd**

Assisted in the establishment and development of microbiological lab for Arch Suzhou, executed lab daily management with setting up documentary standard operation procedures and test methods; maintained equipments for effective function; trained new lab staff

Provided technical support for business departments: implemented microbiological tests for customs and evaluated product performance; followed up the business development according to the tests; built up the data library for local technical service

Developed and evaluated QA test methods; implemented chemical tests for in-process and final products (eg. Zinc Omadine, Copper Omadine), and analyzed results

10/2005 **Trainee, Tsukuba Lab, Arch Chemicals (Japan)**

Obtained microbiological lab establishment information and microbiological experimental skills training

02/2005-06/2005 Research Assistant, TEM Lab of Nanjing University

Synthesized leaflike Bi_2S_3 nanorods with microwave-hydrothermal method, and characterized products with Transmission electron microscopy (TEM)

09/2004 Intern, Nanjing Chem. Corp. Chemical Plant, Nanjing

Studied chemical engineering processes

Publications and Manuscripts in Preparation

1. LeBlanc, G.; **Chen, G.** P.; Jennings, G. K.; Cliffel, D. E., Photoreduction of Catalytic Platinum Particles Using Immobilized Multilayers of Photosystem I. *Langmuir* **2012,** *28* (21), 7952-7956.

2. LeBlanc, G.; **Chen, G.;** Gizzie, E. A.; Jennings, G. K.; Cliffel, D. E., Enhanced Photocurrents of Photosystem I Films on p-Doped Silicon. *Adv. Mater.* **2012,** *24* (44), 5959-62.

3. **Chen, G.;** LeBlanc, G. ; Jennings, G.; Cliffel, D., Electrochemical Investigation on the Impact of Various Redox Mediators on the Photoresponse of a Photosystem I Modified Electrode (submitted to *Journal of Electrochemical Society*)

4. **Chen, G.;** Hijazi, F.; LeBlanc, G. ; Cliffel, D., Probing Nanoscale photodiode photosystem I with Scanning Electrochemical Microscopy (intend to submit to *ACS Applied Materials & Interfaces*)

5. **Chen, G.;** Crisostomo D,; Kimmel, D,; McNees, R.; Elliott, S.; Cliffel, D., Study the dissimilaroty metal reduction pathways of *Shewanella* with spatial resolution by Scanning Electrochemical Microscopy (In preparation)

Conference Presentation & Poster

1. **Chen, G.;** Hijazi, F.; Cliffel, D., Quantitative Electrochemical Study of Surface Immobilized Photosystem I Using Scanning Electrochemical Microscopy, *SEAC poster section, Pittcon*, Atlanta, March 2011

2. **Chen, G.;** LeBlanc, G.; Cliffel, D., Electrochemical Investigation on the Impact of Various Redox Mediators on the Photoresponse of a Photosystem I Modified Electrode, *Electrochemical Energy Summit, 220th ECS Meeting,* Boston, October 2011

3. **Chen, G.;** LeBlanc, G.; Cliffel, D., Investigation of the Catalytic Activity for Hydrogen Production on Platinized Multilayer Films Photosystem I with Scanning Electrochemical Microscopy *Pittcon*, Orlando, March 2012

Awards and Certificates

Auto CAD (certificated)

ISO 9001:2000 Internal Auditor (SGS certificate)

Qualification of technicians in charge of Quality-Inspection of Pharmaceuticals

International Registered/Professional Nutrition Expert

2005 Excellent Graduate Award of Nanjing University

2004 Third-class People's Scholarship

2003-2004 Excellent League Leader of Chemistry Department

Scientific and Professional Skills

QA/QC Chemical techniques:

Atomic Absorption spectrophotometer	Multi-function Infrared Moisture Analyzer
Ultraviolet-Visible Spectrophotometer	HORIBA Laser Particle Size Analyzer
Gardner Color Comparator	Hegman Fineness Gauge
Auto Potentiometric Titrator	ISO 9001:2000

Microbiological techniques:

Wet State Preservation test	Centrifuge
Minimal Inhibition Concentration test	Microscope
ATP (Hygiene monitoring devices) test	

Electrochemical Analysis:

Scanning Electrochemical Microscope	Electrochemical Potentiostat

Surface Analysis:

Materials Printer	Sputter Coater
Langmuir-Blodgett technique	Ellipsometry
Scanning Electron Microscopy	Profilometr
Energy Dispersive X-ray Analysis	

Professional Memberships

The American Chemical Society
The Electrochemical Society
The Society for Electroanalytical Chemistry

References

Dr. David E. Cliffel, Associate Professor of Chemistry
Phone: (615) 343-3937
E-mail: d.cliffel@vanderbilt.edu

Dr. G. Kane Jennings, Professor of Chemical & Biomolecular Engineering
Phone: (615)322-2707
E-mail: kane.g.jennings@Vanderbilt.Edu